

**RELEASE OF ATP FROM HIPPOCAMPAL SLICES DURING
SPREADING DEPRESSION**

A Thesis Submitted to the College of
Graduate Studies and Research
in Partial Fulfillment of the Requirements
for the Degree of Master of Science
in the Department of Physiology
University of Saskatchewan
Saskatoon

by

Anna L. Pozdniakova

Spring 2000

© Copyright Anna L. Pozdniakova, 1999. All rights reserved.

302 001256318

PERMISSION OF USE STATEMENT

In presenting this thesis in partial fulfillment of the requirements for a Postgraduate degree from the University of Saskatchewan, I agree that the Libraries of this University may make it freely available for inspection. I further agree that permission for copying of this thesis in any manner, whole or in part, for scholarly purposes may be granted by the professor who supervised my thesis work, or in his absence, by the Head of Department or Dean of the College in which my thesis work was done. It is understood that any copying or publication or use of this thesis or parts thereof for financial gain shall not be allowed without my written permission. It is also understood that due recognition shall be given to me and to the University of Saskatchewan in any scholarly use which may be made of any material in my thesis.

Requests for permission to copy or to make other use of material in this thesis in whole or in part should be addressed to

Head of the Department of Physiology

University of Saskatchewan

Saskatoon, Saskatchewan S7N 0W0

ABSTRACT

A SD wave represents a short lasting and reversible breakdown of ion gradients in brain cells. These waves occur only in brain tissue and are, therefore, a hallmark of this tissue. SD waves radiate out of the damaged ischemic core into the penumbra and healthy tissue. In the penumbra propagation of SD waves may lead to irreversible damage of brain cells. In healthy tissue SD waves activate microglial cells, the resident macrophage cells of the brain. The signaling pathways leading to activation of microglia are not known. It is known that extracellular ATP is a powerful activator of microglial cells. If ATP is released during SD waves it might be an evidence that ATP serves as a signal for transformation of microglia from resting to activated form. Our experiments were designed to find out whether ATP is released during SD wave.

SD waves were artificially elicited in the rat hippocampal slices (400 μm) by bath application of 100 μM ouabain or by micro-injection of 1.2 M KCl into stratum radiatum of the CA1 region. Ouabain triggered SD waves with an amplitude 6.5 ± 5.2 mV and a duration 11.4 ± 5.2 min that appeared with a 7.5 ± 2.8 min delay after switching normal solution to the solution containing ouabain. The ATP outflow from six slices was measured in the perfusate samples collected before and after application of ouabain. The concentration of ATP in the samples was determined with a luciferase-luciferin system. The basal outflow from six slices averaged 3.3 ± 1.6 pmol/slice/min. Ouabain caused a transient overflow of ATP 10.4 ± 4.4

pmol/slice/min. The increase in ATP outflow started before the appearance of the SD wave. The experiments failed to determine the ATP release from a single hippocampal slice during SD wave elicited by micro-injection of high KCl. The sensitivity of luciferin-luciferase system was not sufficient for determination of the ATP concentration in the perfusate samples collected before, during and after SD wave. Manipulations involving slow-down of the rate of ATP hydrolysis by ecto enzymes, improvement of the experimental chamber, and concentration of the perfusate samples did not improve the sensitivity.

In a separate set of experiments it was demonstrated that approximately 2/3 of extracellular ATP injected into the hippocampal slice were hydrolyzed by nonspecific phosphatases and ectonucleotidases. The observed increase of the ATP release during ouabain-evoked SD wave is not definitive evidence that SD waves cause the release of ATP, because of the possibility that ouabain by itself rather than SD might cause the release of the ATP.

ACKNOWLEDGEMENTS

I am grateful to Dr. W. Walz, my supervisor, and Advisory Committee members for their guidance. I would like to thank Dr. D. Chedrese for the permission to use the equipment and for discussions. I thank Dr. D. Schreyer for interesting questions and corrections.

The animal use protocol for the project was approved by the University of Saskatchewan Animal Care Committee.

TABLE OF CONTENTS

PERMISSION TO USE STATEMENT.....	i
ABSTRACT.....	ii
ACKNOWLEDGEMENTS.....	iv
TABLE OF CONTENTS.....	v
LIST OF FIGURES.....	ix
LIST OF ABBREVIATIONS.....	ix
1. INTRODUCTION.....	1
1.1 Ischemic Core and Penumbra.....	2
1.2 Spreading Depression.....	4
1.3 Ion Channels Involved in SD.....	6
1.4 Metabolic Changes Involved in SD.....	7
1.5 Blood Flow Changes Associated with SD.....	10
1.6 Triggering and Propagation of SD.....	11
1.7 SD in Focal Ischemia.....	13
1.8 Neuroprotective Effects of SD.....	15
1.9 Microglia and Extracellular ATP.....	17
1.10 ATP Release by Brain Cells.....	23
1.11 Release of ATP from Tissues Under Different Experimental Conditions.....	26
1.12 Rationale and Objectives for Present Investigation.....	30

2. MATERIALS AND METHODS.....	32
2.1 Rat Hippocampal Slices.....	32
2.2 Assay of ATP.....	32
2.2.1 Luciferin-luciferase system.....	32
2.2.2 Technical procedure.....	33
2.2.3 Luminescent measurements.....	34
2.3 Electrophysiological Setup.....	34
2.3.1 SD recording.....	34
2.3.2 SD triggering.....	35
2.3.3 Brain slice chambers and ATP sampling.....	36
2.4 Lyophilization of Samples.....	37
2.5 Experimental Protocols and Solutions.....	37
2.5.1 SD in hippocampal brain slices.....	37
2.5.2 ATP dilution in the slice chambers	39
2.5.3 Hydrolysis of ATP by ectonucleotidases and non-specific phosphatases in the slice.....	40
2.5.4 Solutions.....	40
2.6 Data Analysis.....	41
2.7 Statistical Methods.....	42
3. RESULTS.....	43
3.1 ATP Release Caused by Application of Ouabain to Six Hippocampal Slices.....	43
3.2 SD Waves Caused by Application of Ouabain.....	43

3.3 ATP Release from a Single Slice.....	43
3.4 Attempts to Decrease ATP Dilution in the Slice Chamber.....	46
3.5 Hydrolysis of ATP by Ectonucleotidases and Non-specific Phosphatases in Rat Hippocampal Slice.....	50
3.6 Interference of Blockers of Ectonucleotidases and Non-specific Phosphatases with Luciferin-luciferase System.....	50
3.7 Lyophilization of the Samples.....	53
3.8 Effect of DMSO on Sensitivity of Luciferin-luciferase System.....	53
3.9 Luciferase Chemiluminescence and Enzyme Concentration.....	56
4. DISSCUSSION.....	58
4.1 Application of Ouabain Causes ATP release	58
4.2 Attempts to Measure ATP Release from a single slice.....	60
4.3 Is ATP released During SD wave?.....	64
5. CONCLUSIONS.....	70
6. REFERENCES.....	71

LIST OF FIGURES

Figure 2.1	Typical ATP calibration curve.....	38
Figure 3.1	Ouabain triggered ATP release from rat hippocampal slice.....	44
Figure 3.2	SD wave triggered by application of ouabain.....	45
Figure 3.3	SD wave triggered by high potassium.....	47
Figure 3.4	ATP dilution in the chamber of 0.3 ml volume and outflow provided by gravity force.....	48
Figure 3. 5	ATP dilution in the chamber of 0.15 ml volume and outflow provided by a vacuum pump.....	49
Figure 3. 6	Hydrolysis of extracellular ATP by ectonucleotidases and non- specific phosphatases.....	51
Figure 3.7	ATP calibration curves prepared with the ATP standard solutions of different content.....	52
Figure 3.8	ATP calibration curves prepared for standards concentrated 10- fold.....	54
Figure 3.9.	ATP calibration curves prepared fore standards containing DMSO.....	55
Figure 3.10.	Effect of luciferase concentration on the light emission and sensitivity of the assay.....	57

LIST OF ABBREVIATIONS

[³ H]ACh	([³ H]acetylcholine)
[³ H]NA	([³ H]noradrenaline)
[Ca ²⁺] _e	(extracellular Ca ²⁺ concentration)
[Ca ²⁺] _i	(intracellular Ca ²⁺ concentration)
[Cl] _e	(extracellular Cl ⁻ concentration)
[H ⁺] _i	(intracellular H ⁺ concentration)
[K ⁺] _e	(extracellular K ⁺ concentration)
[Na ⁺] _e	(extracellular Na ⁺ concentration)
[Na ⁺] _i	(intracellular Na ⁺ concentration)
4-AP	(4-amino-pyridine)
5-HT	(serotonin)
ACh	(acetylcholine)
ACSF	(artificial cerebral spinal fluid)
AMPA	(α-amino-3-hydroxy-5-methyl-4-isoxazolepropionate)
ATP	(adenosine triphosphate)
BG	(background)
cAMP	(cyclic adenosine monophosphate)
CBF	(cerebral blood flow)
CNS	(central nervous system)

CPP	(3-((±)-2-carboxypiperazine-4-yl)-propyl-1-phosphonic acid)
CSF	(cerebral spinal fluid)
DMSO	(dimethyl sulfoxide)
DNQX	(6,7-dinitroquinoline-2,3-dione)
DTT	(dithiothreitol)
EDTA	(ethelenediaminetetraacetic acid)
GFAP	(glial fibrillary acidic protein)
HPLC	(high-pressure liquid chromatography)
I	(current)
IL-1 β	(interleukin-1 β)
MCA	(the middle cerebral artery)
MK-801	(dizocilpine maleate)
NADH	(nicotinamide adenine dinucleotide)
NMDA	(N-methyl-D-aspartate)
NO	(nitric oxide)
NPPB	(5-nitro-2(3-phenylpropylamino)benzoic acid)
RLU	(relative light units)
SD	(spreading depression)
TEA	(tetraethylammonium)
Tricine	(N-tris-[hydroxymethyl]methylglycine)
TTX	(tetrodotoxin)
V	(voltage)
VSOAC _s	(volume-sensitive organic anion channels)

1. INTRODUCTION

A stroke lesion usually consists of a densely ischemic core and perifocal areas (the penumbra) in which neurons die with a delay of days. The penumbral areas were originally defined as intermediate zones having a reduction in CBF to a level that interrupts neuronal electrical activities, yet permits maintenance of membrane pumps and preservation of ion gradients (Hakim, 1987). The penumbra has potential clinical potency. The interruption of neural activity in this zone is reversible but there is a limited time window for this. Within the first hours after ischemia depolarizations named SD waves originating from ischemic foci travel over the penumbra and the entire hemisphere. In the penumbra where the cells are compromised metabolically SD waves generate a transient mismatch between energy supplies and demand. The gradual depletion of tissue ATP and high energy phosphate reserves following repetitive SD waves may eventually lead to perinfarct tissue death (Hossmann, 1994). The infarction output may be significantly decreased pharmacologically with gap junction blockers or non-competitive NMDA receptor antagonist MK-801 (Nedergaard, 1996) which inhibits propagation of SD waves.

In the healthy tissue with normal blood flow artificially elicited SD waves are harmless and might have a neuroprotective effect. They cause activation of astrocytes and microglia. Microglia are resident brain macrophages that strongly respond to cerebral ischemia (Lehrmann et al., 1997; Schroeter et al., 1999). Upon

activation microglia undergo morphological changes and finally become indistinguishable from macrophages both morphologically and in their expression of surface and intracellular antigens. Activated microglia can produce neurotoxic mediators as well as neurotrophic factors (Wood, 1995). Mechanisms underlying transformation of the resting microglia to the activated form are not known. The involvement of P2 purinergic receptors is proposed (Walz et al., 1993). Microglial cells express several subtypes of purinoreceptors which induce various membrane conductances and changes in cytoplasmic Ca^{2+} concentration when they are activated by extracellular ATP (Inoue, 1998). During focal ischemia ATP may leak out of damaged neurons and glial cells and be a signal for functional changes in microglial cells in the lesion area. Microglia are also activated in the remote morphologically intact brain areas covered by SD (Schroeter et al., 1999) triggered by focal ischemia (Dietrich et al., 1994). What is a signal for remote microglial responses after focal ischemia? There is a suggestion that in the morphologically intact brain areas microglia are activated by ATP which is released via SD waves propagating from the infarction areas.

1.1 Ischemic Core and Penumbra.

Ischemic stroke is a cerebrovascular accident caused by the reduction of blood supply as a result of a blood clot or rupture of a vessel (Sweeney et al., 1995). The artery most often occluded is the middle cerebral artery (MCA). Occlusion of MCA causes nearly complete ischemia in the center of the vascular territory. This ischemic region has very low local cerebral blood flow (CBF) ($< 10 \text{ ml/100 g/min}$)

(Hossmann, 1994) and rapidly becomes irreversibly damaged. Within seconds neuronal electrical activity fails and within a few minutes ATP synthesis stops and ion pumps fail. Membrane ion pump failure causes membrane depolarization and increase in extracellular potassium concentration. Glutamate release becomes unregulated. High concentrations of extracellular glutamate activate NMDA and AMPA receptor channels, causing them to open and allowing massive Ca^{2+} influx (Sweeney et al., 1995) that disrupts intracellular processes killing neurons. All cells within this region of low blood flow referred to as the ischemic core undergo necrosis.

The ischemic core is surrounded by tissue with reduced CBF (approximately 15 to 40 ml/100 g/min). This zone of mild to moderately reduced CBF relates to the concept of the ischemic penumbra (Astrup et al., 1981). Cells in the penumbra are not necessarily lost but can survive if blood flow is restored. Hossmann (1994) defined penumbra as “a region of constrained blood supply in which energy metabolism is preserved”. Ischemic brain tissue of the penumbra has enough energy to survive for a short time but not enough to communicate and function (Hakim, 1998). Cells are alive but synaptic transmission is abolished, oxidative metabolism is reduced and the rate of ion pumping is decreased. The residual perfusion supplies enough oxygen to maintain tissue concentration of ATP close to normal. Thus there is no complete ion pump failure and extracellular potassium concentration is normal or only slightly elevated (Astrup et al., 1977). Intracellular calcium levels are raised from 100 nM to about 200 nM, a value that is not detrimental to the cell (Collins et al., 1991). This region remains viable for only one or perhaps a few hours after

vascular occlusion and can be reactivated by raising the blood flow (Memezawa et al., 1992). If blood flow is not restored tissue infarction develops. The mechanism by which the penumbra evolves into infarction and the factors which determine whether the penumbra can be salvaged still remain uncertain. There are two major hypothesis concerning the mechanism causing penumbral tissue death. The first hypothesis is that ischemic cell death is caused by neurotoxic mechanisms in a non-wave-dependent manner. The proposed mechanisms include the generation of oxygen free radicals and nitric oxide, and the initiation of apoptosis. The main proposed mechanism is excitotoxicity suggesting that the massive release of excitatory amino acids, such as glutamate and glycine, from the dying tissue in the center of the infarct core spread outward due to diffusion and can damage adjacent and distant cells by promoting intracellular calcium accumulation. The levels of extracellular glutamate in the penumbra may increase 25-fold because of depression of glutamate uptake processes due to energy deficiency in this region. The second theory is that the expansion of tissue injury into the penumbra zone is caused by the progression of spreading depression-like depolarizations that have been found in ischemic tissue. SD waves originate from the core of an infarct and propagate outward into the penumbra activating a cascade of metabolic events that eventually lead to penumbra tissue death (Ruppin et al., 1999).

1.2 Spreading Depression.

SD was discovered by Leao (1944) as a dramatic transient disturbance of brain function in a response to a variety of noxious influences. SD is one of the most

reproducible electrophysiological phenomena in CNS gray matter and can be evoked by a massive depolarization caused by K^+ , the excitatory amino acid glutamate or by electric or mechanical stimulation (Bures et al., 1974). SD is a slowly propagating (1.5-7.5 mm/min) extracellular negative wave (10-35 mV) that is accompanied by depolarization of both astrocytes and neurons to approximately 0 mV (Somjen et al., 1991). Within 1-3 min the cells repolarize and then may be hyperpolarized for a few minutes. During the peak of the membrane depolarization neurons are unexcitable but before and afterward increased spiking occurs (Higachida et al., 1974).

Using methods based on continuous determination of the extracellular concentration of extracellular markers and light scattering the decrease of the size of the extracellular space to 50% during SD was shown (Hansen and Olsen, 1980; Snow et al., 1983). The finding of large decreases of brain extracellular space is in agreement with the results of the study of a drastic redistribution of ions between the intra- and extracellular spaces accompanying the SD process. K^+ ions flow out of cells and Na^+ , Cl^- , Ca^{2+} , and water flow into cells causing cellular swelling (Hansen and Zeuthen, 1981; Holthoff and Witte, 1996).

During the SD extracellular K^+ concentration increases greatly in two phases. In the first it rises slowly from the resting value of 3.1 mM to a level of 11 mM within about 2 min. In the second period extracellular K^+ concentration rises to 60-70 mM within seconds accompanied by an abrupt negative change of the extracellular potential. The maximum level of extracellular potassium concentration is maintained for about 20 s and declines at a comparatively slow rate (Hansen and

Zeuthen, 1981; Somjen et al., 1992). After 40 s K^+ level has returned to its normal concentration, sometimes undershooting the control level during the next 1-2 min. The SD-related extracellular potential shifts have the pattern of change similar to the changes in extracellular K^+ concentration (Nedergaard, 1996).

The ionic changes that occur during SD involve the decrease in extracellular Ca^{2+} , Na^+ , and Cl^- concentrations. The decrease in $[Ca^{2+}]_e$ began with a slight delay relative to the increase of $[K^+]_e$ (Kraig and Nicholson, 1978; Herreras and Somjen, 1993). The minimum level to which $[Ca^{2+}]_e$ fell is up to 100 times lower than its resting concentration. The decrease of $[Na^+]_e$ is not so drastic, reaching its minimal level of 65-75 mM. Following the changes of extracellular potential, $[Ca^{2+}]_e$ and $[Na^+]_e$ recover in two phases. Finally $[Ca^{2+}]_e$ and $[Na^+]_e$ return to their normal levels after several-minute delay comparing with extracellular potential and $[K^+]_e$. The changes in $[Cl^-]_e$ have a similar pattern. $[Cl^-]_e$ decrease to 90 mM and then reach the pre-SD level with a delay. Thus the changes of ion concentrations do not start at the same time in SD. The rise in $[K^+]_e$ precedes the decrease of $[Ca^{2+}]_e$, $[Na^+]_e$, and $[Cl^-]_e$. These changes indicate the intracellular movements of Na, Cl and Ca, and extrusion of K from the cells during SD (Hansen and Zeuthen, 1981).

1.3 Ion Channels Involved in SD.

The identity of the channels through which ions move during SD has remained uncertain. There is a severe loss of membrane resistance that is consistent with the SD-related depolarization of neurons and with the redistribution of ions (Haglund and Schwartzkroin, 1990; Somjen et al., 1992). The entire I-V function becomes a

straight line reflecting independence of membrane resistance from voltage. This loss of membrane resistance during SD could be because of nonspecific transient breakdown of the membrane, but it was found that ions larger than 1.12 nm can not enter cells during SD. Thus anion permeable channels that become active during SD are bounded in size (Phillips and Nicholson, 1979).

Certain selective ion channels may be involved in the SD phenomenon. In the presence of TEA the membrane potential shifts and changes of $[K^+]_e$ are consistently reduced indicating that during SD some of the K^+ ions escape from cells through voltage-gated potassium channels. 4-AP does not have such an effect. Therefore not all voltage-gated potassium channels participate (Aitken et al., 1991). TTX, a potent blocker of the sodium channels involved in the classical action potential, does not produce any significant reduction in the $[Na^+]_e$ variation during SD. Therefore voltage sensitive Na^+ channels have little or no role in the depolarization (Tobiasz and Nicholson, 1982).

A severe drop in extracellular Ca^{2+} concentration during SD is presumably because of movement of Ca^{2+} into the cells. Ca^{2+} ions can enter neurons via voltage-gated channels and also via NMDA receptor coupled channels. Blockade of voltage-gated Ca^{2+} channels with either Co^{2+} or Ni^{2+} and glutamate receptor coupled channels with CPP and DNQX lessens, but does not prevent, the drop in $[Ca^{2+}]_e$ (Jing et al., 1993). Therefore during SD some but not all of Ca^{2+} that flows into the cell pass through voltage-gated or glutamate-linked channels.

Particular involvement of voltage-gated K^+ , Ca^{2+} and glutamate receptor coupled Ca^{2+} channels in the SD phenomenon cannot explain all changes in

extracellular ion concentrations and the SD-related depolarizations. The permeability mechanism that becomes active during SD remains unknown.

1.4 Metabolic Changes During SD.

The SD effects on the membrane potential and ion concentration shifts are reversible. After 1-2 min the ion gradients and membrane potential return to pre-SD levels (Somjen et al., 1993). This normalization is responsible for metabolic activation in the brain tissue. The increase of energy demand leads to the expense of endogenous energy stores and a large elevation of glucose utilization.

The onset of SD changes the ATP content in brain tissue. When the negative shift in extracellular SD potential reaches its maximum ATP values decrease to 54 – 60% (Csiba et al., 1985; Guat et al, 1994) and gradually returns to normal after restoration of membrane potential. The phosphocreatine values are most sensitive to the SD. Concentration of phosphocreatine drops to 24% of control at the crest of the SD wave. The decrease in high-energy phosphates during the phase of cellular depolarization is accounted for the fact that the energy-dependent processes remain activated during the liberation of potassium and calcium influx. A depression in high-energy phosphates leads to the activation of glucose metabolism.

During and after SD cerebral glucose utilization is markedly increased in most areas of the cerebral cortex (Shinohara et al., 1979; Gjedde et al., 1981). Migration of a single SD wave is accompanied by a decrease in glucose content to 72% of control (Mies and Paschen, 1984). After restoration of membrane potential cortical

glucose concentrations remain of 60% of the control value (Csiba et al., 1985). The steep negative shift in the extracellular potential during SD is paralleled by a significant decrease in tissue pH from 7.20 to 6.85 (Csiba et al., 1985; Chesler and Kraig, 1989; Guat et al., 1994), which occurs almost concomitantly with a significant reduction in cortical glucose content. During the restitution of the membrane potential cortical tissue pH decreases to 6.75 (Csiba et al., 1985). At the same time lactate values increase to approximately 200% of the control values (Gualt et al., 1994). The rapid development of cortical tissue acidosis which occurs together with the reduction in tissue glucose and lactate accumulation possibly indicate a partial involvement of anaerobic glycolysis during SD (Busa and Nuccitelli, 1984).

As a result of activation of energy-dependent processes in the cells the mitochondria are activated in order to produce the extra ATP needed and the oxidative metabolic activity is increased (Lothman et al., 1975). There is a correlation between the oxidation of NADH and extracellular potassium during SD that suggests a substantial expenditure of energy for the pumping of K^+ by the ATPases back from the extracellular space. Ouabain significantly decreases the oxidation rate stimulated by the rising ADP concentration due to the breakdown of ATP by the ouabain-sensitive Na,K-pumps (LaManna and Rosental, 1975).

1.5 Blood Flow Changes Associated with SD.

Large changes in the oxidative metabolic activity during SD are accompanied by changes in blood flow. In order to produce the extra ATP and keep the balance of oxygen in the normal range for oxidation of NADH, activated mitochondria need influx of the metabolic substrates glucose and O_2 .

SD induces arteriolar dilation resulting in an increased cerebral blood flow with approximately one minute delay after the onset of the SD wave (Hansen et al., 1980; Shibata et al., 1990). The cortical blood flow remains unchanged at the first minute while the $[K^+]_e$ increase to 60 mM. High cerebral blood flow is not directly associated with the increased $[K^+]_e$ but rather with the subsequent reduction of $[K^+]_e$. During this phase cortical blood flow increases to twice the normal value while $[K^+]_e$ returns to 3 mM (Hansen et al., 1980). The mechanisms that couple increased cerebral blood flow to increased metabolic activity during SD are not fully understood, but they appear to involve synthesis and/or release of nitric oxide (Colonna et al., 1994; Goadsby et al., 1992), prostaglandins (Shibata et al., 1990) and calcitonin gene related peptide which dilate the blood vessels due to activation of receptors on vascular smooth muscle cells and increased intracellular levels of cAMP (Colonna et al., 1994). The increase of cerebral blood flow is coupled to an increase of glucose transport from blood to brain. The spread of SD wave is consistent with a threefold increase of the consumption of glucose and the consequent increase of net transfer of glucose from blood to brain (Gjedde et al., 1981).

Propagation of SD induces dramatic dilation of the vessels; however, the dilation is followed by a prolonged constriction of the vessels after SD expiration (Shibata et al., 1991). Recovery from SD-induced vascular changes is relatively rapid and complete (Busija and Meng, 1993).

1.6 Triggering and Propagation of SD Waves.

The mechanisms of triggering and propagation of SD waves are not clear. Experimentally SD may be evoked by depolarization of a critical mass of cortical tissue, by K^+ or glutamate, by mechanical or electric stimulation (Nedergaard, 1996). SD spreads like a wave from its site of origin across the cortex with a velocity of about 2-5 mm/min. Both elicitation and propagation of SD are sensitive to competitive and noncompetitive antagonists of NMDA receptor complex (Sheardown, 1993; Nedergaard, 1996). The NMDA antagonists increase SD threshold, decrease the propagation velocity, decrease the duration of the accompanying extracellular potential, K^+ and Ca^{2+} changes and may completely inhibit SD propagation (Marrannes et al., 1988). The fact that K^+ -induced release of glutamate and SD initiation require the presence of extracellular Ca^{2+} suggests that glutamate is transiently released from presynaptic vesicles during SD (Obrenovitch et al., 1996). However, a high extracellular level of glutamate is not the driving force sustaining cortical SD propagation. Glutamate, required for NMDA receptor activation is released very locally at the synaptic level and provides Ca^{2+} influx through NMDA-activated ionophores that is essential to SD propagation. Local, high

extracellular concentration of K^+ remains the plausible trigger of SD (Obrenovitch and Zilkha, 1995).

Glial cells seem to contribute to SD. Glial depolarization of 20-40 mV during SD is monophasic and slow, lasting 2.5, min while neuron depolarization is a bimodal type: rapid depolarization with burst discharges and slow depolarization with no spike lasting 5-6 min. Both cells are integral factors in SD (Higashida et al., 1974). However the relative participation of glia and neurons in SD remain obscure. The glial specific metabolic poison fluorocitrate causes a rapid impairment of glial function and decrease of glial membrane potential but does not hinder SD propagation but rather favors it (Largo et al., 1997). SD waves propagate faster and last longer and are able to spread into hippocampus after being provoked in neocortex. Only when neuronal function fails do SD waves fail to enter the region of fluorocitrate treatment. According to these results, neurons are the major generator of SD while an energy shortage in glial cells makes brain tissue more susceptible to SD.

Whether or not glia are the cells that propagate SD is still not understood. SD propagation may be mediated by the release of a substance from cells into extracellular space or by the intercellular transfer of a signal through a network connected by gap junctions between neurons or glial cells. Waves of SD were blocked by different inhibitors of gap junctional coupling such as halothane, and the long-chain alcohols heptanol, hexanol and octanol (Nedergaard et al., 1995; Largo et al., 1997). A number of investigators have proposed that glial cells, which are believed to be normally more profusely joined by gap junctions than neurons, are

the cell type primary responsible for generating SD. Ca^{2+} -waves that can propagate among cultured astrocytes could be related to SD phenomena, but there is no evidence so far to establish this relation. Ca^{2+} -waves may spread without indications of SD occurrence (Dani et al., 1992). Also the fact that heptanol succeeds in blocking SD propagation while fluorocitrate fails in the same rat hippocampal tissue slices is compatible with the idea that normally functioning glial cells are not essential for SD generation or propagation. Largo et al. (1997) proposed that neuronal gap junctions that are required for SD propagation need not be open normally but must be able to open during SD propagation. Their conclusion that glial cells are not essential for SD propagation does not take into account that the glial gap junctions could continue to function even if the energy metabolism of the cells is impaired and their membrane potential is reduced or abolished. Thus, the mechanisms of triggering and propagation of SD waves are still unknown.

1.7 Spreading Depression in Focal Ischemia.

The mechanisms by which focal ischemia evolves into infarction are still unsettled. If left untreated the necrotic infarct zone will progressively expand into the penumbra in which there is metabolically compromised tissue and marginal blood flow. Understanding the mechanisms underlying tissue damage in the ischemic penumbra may be helpful in designing therapeutic strategies for acute ischemic stroke. Hossmann (1994) suggested that the reason for the expansion of irreversible tissue injury into the penumbra zone is occurrence of SD waves. As first

described by Nedergaard and Astrup (1986) SD waves are generated spontaneously in focal stroke. SD waves originate from two sources: the evolving infarct itself, where persistent elevated levels of $[K^+]_e$ and glutamate, and transient ischemic foci within the poorly perfused penumbra. The evoked SD waves spread radially through the penumbra into the peripheral zone with healthy tissue and normal blood flow (Nedergaard and Hansen, 1993). The duration of SD waves in the penumbra is longer than in the intact brain tissue. Its prolonged duration may reflect that the depleted energy state of penumbra increases the time to restore ion gradients by active ion transport. During SD the energy demands are greatly enhanced and the metabolic rate of tissue increases in response to the activation of ion exchange pumps. In the healthy tissue with normal blood supply the increase in glucose and oxygen demands is coupled to a parallel increase of blood flow. This mechanism is suppressed in the peri-infarct penumbra because of the reduced capacity of the pial collateral vascular system supporting perfusion in the penumbra. The result is a misrelationship between the increased metabolic demands and the low oxygen and glucose supply (Hossmann, 1994).

The pathogenetic role of SD waves for the progression of ischemic injury is supported by the close linear correlation between the number of SD waves and infarct volume (Mies et al., 1993). Correlation analysis of this relationship showed that during the initial 3 hours of vascular occlusion each SD wave increased the infarct volume by more than 20%. Later, Takano et al. (1996) demonstrated that ischemia-related and induced SD waves significantly increased ischemic volume. This is the reason why any suppression of SD reduces the volume of brain infarcts.

Hyperglycemia reduces the number of SD waves and depresses their migration. In hyperglycemic rats neuronal loss around the penumbra is reduced or absent (Nedergaard and Diemer, 1987; Nedergaard, 1996). Reduction in body temperature during focal ischemia results in a reduction of infarct size. The volume of infarct in hypothermic rats is significantly less than in normothermic or hyperthermic animals. The decrease in infarct volume strongly correlates with the number of SD waves spontaneously evoked during ischemia (Chen et al., 1993). Pharmacological suppression of SD waves by a gap junction blocker octanol reduces infarct volume following middle cerebral artery occlusion in rats by 60% (Rawanduzy et al., 1997). The NMDA receptor antagonist causes parallel reductions in the number of SD waves and in volume of infarction (Nedergaard, 1996).

Collectively, these data support the hypothesis that SD contributes to expansion of ischemic damage. Waves of SD, generated in ischemic tissue, migrate to the penumbra where they deplete the cellular energy stores. Finally tissue in the penumbra is not able to repolarize after invasion of SD, but remains depolarized and is eventually incorporated into the infarct volume.

1.8 Neuroprotective Effects of Spreading Depression.

SD waves propagated in normal brain do not induce irreversible neuronal injury (Nedergaard and Hansen, 1988). Moreover, SD could be used as a preconditioning treatment leading to the “ischemic tolerance” phenomena. In rats, SD elicited by application of 2M KCl for 2 h, induced tolerance of cortical neurons to a subsequent episode of ischemia. The number of necrotic neurons in the cerebral

cortex ipsilateral to the application of KCl was significantly smaller than that in contralateral cortex (Kobayashi et al., 1995). A neuroprotective action of SD was also shown by Matsushima et al. (1996). SD waves elicited for 2 hours three days before middle cerebral artery occlusion caused reduction of neocortical infarct volume.

SD may be involved in the induction of ischemic tolerance by acting on astrocytes and microglia. Experimentally elicited SD waves caused reactive gliosis which might have a neuroprotective effect (Jabs et al., 1999). Astrocytes became activated and expressed an increase in GFAP staining after 13-37 neocortical SD waves evoked in rats by application of KCl for 3 hours. SD waves were associated with a significant, 43% increase in GFAP staining intensity which remained greater than normal for more than 2 weeks (Kraig et al., 1991). Astroglial response also occurred in photochemically induced focal ischemia of the rat cerebral cortex. During the first 2 hours after photothrombosis 5-7 SD waves could be detected on the cortical surface. They caused a transient astrocytic reaction, remote from the lesion and effecting the entire ipsilateral cortex. Astrocytes responded to SD waves by increased expression of GFAP, observed beginning on day 3 after focal ischemia. Remote astrocytic activation was completely abolished with inhibition of SD waves by non-competitive NMDA-receptor antagonist MK-801, while the reaction in the border zone of the infarct remained unchanged (Schroeter et al., 1995). Thus, SD triggered the cellular mechanisms that induced the transformation of normal astrocytes into reactive ones.

There is evidence that microglia are activated by SD waves. SD waves elicited for one hour by the application of KCl were sufficient to activate microglial cells throughout the cortex at 24 hours. Activated microglial cells showed a striking de-novo expression of major histocompatibility complex class II antigens. Microglial activation was not correlated with histologically detectable neuronal damage. No microglial reaction was found in the cortex of sham-operated animals (Gehrmann et al., 1993).

1.9 Microglia and Extracellular ATP.

Microglial cells are found throughout the brain and comprise 10-20% of all glial cells (Altman, 1994). They lie between neurons in the gray matter and parallel to axons in the white matter. Numerous pathological events in the brain trigger a response in microglial cells, which rapidly transform from a resting state to an activated form. The activation of microglia includes immunological, metabolic and morphological changes. Activated microglia divide, become amoeboid and motile, and can move to the site of injury or surround affected neurons. Activated microglia are mainly scavenger cells but also perform various other functions in tissue repair and neuronal regeneration. They are able to upregulate many protein species and release cytokines (e.g. interleukin-1 and -6) and growth factors (Gehrmann et al., 1995). Proliferating microglia show increased expression of major histocompatibility complex class I and II immunomolecules at their surfaces and finally transform into a phenotype indistinguishable from a phagocytic macrophage. The pathways of the long-term changes of microglia gene expression and the

reorganization of the cell phenotype following the immediate changes in the brain microenvironment are yet unknown. They might be associated with specific plasmalemmal receptors (Haas et al., 1996). It has been found that microglia express receptors for ATP, G-protein coupled-type P2 receptors such as P2Y and ionotropic P2 receptors such as P2Z also named P2X7 (Ferrari et al., 1996). The activation of these receptors by ATP induces depolarizations and a variety of conductances as well as changes in cytoplasmic Ca^{2+} concentration in microglial cells.

A number of studies have examined the effects of ATP on electrophysiological properties of microglia. The primary findings were that ATP acted on P2 purinoreceptors to induce two different current components in mouse or rat microglia. The first component was associated with activation of a non-selective cation channel with permeability to inward Na^+ and outward K^+ . The second current component had a delayed onset and was selective for outward K^+ current. The activation of the P2 purinergic receptor was accompanied by an increase of cytosolic Ca^{2+} , which could act as a signal for differentiation of resting microglia into fully activated macrophages through a number of transitional states (Walz et al., 1993).

ATP evokes currents in proliferating and non-proliferating rat microglial cells by stimulating purinoceptors of the P2Y type. Activation of P2Y receptors led to the opening of non-selective cationic channels that were permeable not only to Na^+ but also to Ca^{2+} . Thus ATP was able to permeabilize the plasma membrane of rat microglial cells to cations in a manner similar to the effects of ATP on plasma membranes of rat and mouse peritoneal macrophages (Steinberg et al., 1987). The second mode of action of P2Y receptors was the opening of voltage-sensitive,

outwardly rectifying potassium channels that caused the decrease in sensitivity of activated microglia towards the depolarizing, excitatory effect of ATP (Norenberg et al., 1994).

These findings that ATP activates a rapidly desensitizing non-selective cationic conductance followed by a non-desensitizing K⁺ conductance in rat microglia were confirmed by Langosch et al. (1994). It has been reported that rat microglia possess both ATP-sensitive P2Y and adenosine-sensitive P1-purinoceptors. Early inward currents were mediated by P2Y-purinoceptors, while late outward currents were mediated by P2Y or P1-purinoceptors (Langosch et al., 1994).

ATP currents have also been recorded from microglial cells harvested from the surface of corpus callosum slices acutely isolated from the mouse brain. At a concentration of 1 mM, ATP triggered the generation of a complex membrane current comprised of three components. An initial fast inactivating inward current was resulted from the activation of non-specific cationic channels and had a reversal potential at about -20 to -15 mV. The second component was a steady-state current carried mainly by K⁺ ions with reversal potential about -50 to -40 mV. The fast and steady-state components had an activation threshold at 10 μ M ATP, and 100 μ M ATP evoked an almost maximal response. The third component of ATP-induced inward current was associated with activation of non-selective channels and could be observed only while 1 mM ATP was applied. This component could be evoked only by ATP, but not by other purinoceptor agonists suggesting the involvement of the P2Z purinoreceptor, which has been described in macrophages cell lines (Haas et al., 1996).

It is known that changes in cytoplasmic Ca^{2+} concentration are an important cellular signal transduction mechanism. The increase of $[\text{Ca}^{2+}]_i$ results in significant changes of gene expression via the activation of Ca^{2+} /calmodulin-dependent enzymes (Ghosh and Greenberg, 1995). Recently, the primary findings that ATP induced the increase of cytosolic Ca^{2+} in mouse and rat microglial cells (Walz et al., 1993; Norenberg et al., 1994) were confirmed by Toescu et al. (1998). Application of ATP triggered a Ca^{2+} response in microglial cells which involved both Ca^{2+} influx through ionotropic receptors and Ca^{2+} release from intracellular pools. The ionotropic component of the ATP response mediated through the P2X receptors was significantly reduced with the removal of extracellular Ca^{2+} and was sensitive to Ca^{2+} channel blockade. The second component of the ATP-induced $[\text{Ca}^{2+}]_i$ response persisted in Ca^{2+} -free solutions indicating the involvement of intracellular Ca^{2+} release. These results showed that in microglial cells ATP activated two sets of receptors, ionotropic P2X and metabotropic P2Y associated with the initiation of Ca^{2+} release from intracellular stores via inositol-1,4,5-trisphosphate-gated channels. The most intriguing observation in this study was that after the maximal stimulation of the metabotropic P2Y receptors with $100\mu\text{M}$ of ATP in the absence of extracellular Ca^{2+} , the readmission of Ca^{2+} resulted in a transient $[\text{Ca}^{2+}]_i$ elevation which after reaching a peak did not recover to the initial resting level, but approached a new steady-state level that was then maintained for 20 min. The transition to a new resting level led to dramatic changes in $[\text{Ca}^{2+}]_i$ homeostasis. The cytosolic Ca^{2+} became extremely sensitive to extracellular Ca^{2+} concentrations and Ca^{2+} channel blockade. Thus the new resting $[\text{Ca}^{2+}]_i$ level was determined by the

long-term activation of transmembrane Ca^{2+} influx representing a capacitative Ca^{2+} entry pathway. This pathway is activated by the depletion of Ca^{2+} stores. The depletion of Ca^{2+} stores activates a specific set of plasmalemmal Ca^{2+} -permeable channels by poorly characterized factors (Berridge, 1995). The involvement of this pathway might play an important role in triggering a variety of intracellular Ca^{2+} -dependent processes that associated with activation of microglia. An extensive depletion may occur under pathological conditions when several metabotropic receptors are activated simultaneously and may lead to long lasting $[\text{Ca}^{2+}]_i$ elevation (Toescu et al., 1998).

The electrophysiological responses of human microglia to ATP have been studied. The application of ATP (at 0.1 mM) led to the activation of a transient inward non-selective cationic current followed by a transient outward K^+ current. The outward current showed no evident inactivation but despite the continued presence of ATP decreased with time, and by 90 s after the application of ATP had returned to near the control level. The ATP response included an increase in intracellular calcium. The initial transient increase of $[\text{Ca}^{2+}]_i$ reached a peak value near 400 nM. Peak $[\text{Ca}^{2+}]_i$ rapidly decayed to a plateau level significantly higher than baseline of intracellular calcium. The initial transient phase persisted in Ca^{2+} -free media and was due to release of Ca^{2+} from intracellular storage sites. The later plateau phase was consistent with Ca^{2+} influx. These changes in microglial currents and $[\text{Ca}^{2+}]_i$ were not found with elevated external K^+ (at 40 mM), which only increased inward rectifier K^+ conductance, as was observed with ATP (McLarnon et al., 1999).

These data indicated that microglial cells express several subtypes of purinoreceptors which control various membrane conductances. Their activation by extracellular ATP could be a signal triggering functional changes in microglia in response to brain injury when extracellular ATP may appear as a result of leakage from damaged neurons and glial cells.

Microglia which are activated by ATP can release plasminogen, which is thought to be a key molecule for the neurotrophic effect because it promotes the development of mesencephalic dopaminergic neurons and enhances neurite outgrowth from explants of neocortical tissue. Inoue et al. (1998) showed that ATP (10-100 μM) stimulated the release of plasminogen in a concentration-dependent manner during a 10 min stimulation, whereas glutamate (100 μM) did not. It is known that NO is released from various cells following the cascade of Ca^{2+} influx, activation of Ca^{2+} /calmodulin-dependent protein kinase, and activation of NO synthetase. However, neither ATP (100 μM) nor glutamate (100 μM) stimulated the release of NO in these cultured microglial cells. ATP induced a transient increase in the $[\text{Ca}^{2+}]_i$ in a concentration-dependent manner which was totally dependent on $[\text{Ca}^{2+}]_e$ and was a result of activation of the ionotropic P2X7 receptor. Glutamate (100 μM) had no effect on $[\text{Ca}^{2+}]_i$. The data suggested that ATP leaking out of cells damaged by ischemia or trauma mediates signals to microglia, resulting in the stimulation of the release of plasminogen which may modulate the function of the neurons.

Little is known about the function of extracellular ATP in the immune system. ATP-releasing nerve terminals are widely spread throughout CNS and a target for

ATP released by neurons may be microglia which are the CNS counterpart of tissue macrophages. Indeed, strong evidence for an involvement of ATP in IL-1 β release from microglial cells was provided (Ferrari et al., 1996). ATP (5 mM) caused IL-1 β release from wild-type and primary cultures, but not ATP extracellular-resistant mouse microglial cells. The effect was mediated most likely via P2Z receptors. The data suggested a role for extracellular ATP in neuroimmunomodulation.

At present extracellular ATP is considering to be putative agent that is released under different pathological conditions from damaged neurons and serves as an extracellular signal for transformation of microglial cells from a resting to an activated form. Although the physiological role of plasma membrane microglial receptors for extracellular ATP P2Y and P2Z is far from being understood, the involvement of these membrane molecules in the immune and inflammatory reactions is possible.

1.10 ATP Release by Brain Cells.

The function of ATP as an energy source has been known for a long time. The ubiquitous nature of the ATP molecule and the fact that it is rapidly hydrolyzed to adenosine by ectonucleotidases, have made other functions and mechanisms of its release difficult to identify. Since 1970 (Burnstock et al., 1970) the hypothesis of an extracellular role of ATP as a neurotransmitter and/or modulator in the peripheral nervous system has been gaining recognition. Recently a growing number of findings have been accumulated as strong evidence that ATP can act as a fast

excitatory transmitter in a neuro-neuronal synapse in peripheral ganglia and brain (Zimmermann, 1994). The unique features of ATP receptor/channels allowing local influx of calcium into the cell without prior depolarization and the fact that ATP is rapidly hydrolysed by ectonucleotidases to adenosine, which has inhibitory postsynaptic actions causing the opening of potassium channels, give ATP, as a transmitter, properties different from other neurotransmitters in central nervous system (Edwards and Gibb, 1993).

In central neurons ATP is co-stored with transmitters such as ACh, noradrenaline and 5-HT in synaptic vesicles in the millimolar range and is released from nerve terminals with the transmitter by neuronal activity (Zimmermann, 1994; Vizi et al., 1997; Sperlagh et al., 1997; Sperlagh et al., 1998). It is also possible that ATP is stored in separate population of synaptic vesicles within nerve terminals and released in a Ca^{2+} -dependent manner during the process of synaptic modulation (Sperlagh et al., 1996; Sperlagh et al., 1998). ATP is co-released with glutamate in the interneurons innervated by glutamatergic neurons (Inoue et al., 1995).

It has been known for some time that astrocytes release a remarkable amount of purines and represent a very important source of adenine nucleotides and nucleosides in CNS. Cultured astrocytes from rat striatum released purines at rest and during field electrical stimulation. The release was frequency-dependent and a part of the release was Ca^{2+} - and potassium-dependent, suggesting the involvement of these ions in the mechanism by which the purines were released from astrocytes (Caciagli et al., 1988). Recently, the release of a defined nucleotide, ATP, was studied in cultured astrocytes derived from the brain hemispheres of newborn rats.

Cultured astrocytes responded to activation of any of three ionotropic glutamate receptor types, namely NMDA, AMPA and kainate receptors, with release of ATP. There was a basal efflux of ATP, which was increased up to 19-fold by glutamate or its three receptor type-selective agonists. The basal efflux of ATP was not changed by antagonists of glutamate receptors. If neurons release ATP by exocytosis, the mechanism by which ATP crosses the membrane of astrocytes remained unsolved (Queiroz et al., 1997). Recently, Queiroz et al. (1999) have examined the mechanisms that mediate the release of ATP from primary cultures of rat cortical astrocytes in response to glutamate receptor activation. The NMDA and kainate – induced release of ATP required calcium entry which occurs through the ionotropic glutamate receptors themselves and also partly through voltage-dependent calcium channels that are opened by depolarization. This release was not due to neuron-like exocytosis or intracellular ATP transporters occurring in the plasma membrane. The AMPA- induced release did not require extracellular calcium and might involve the inositol phosphate signal transduction pathway because it was abolished by lithium, an inhibitor of inositol monophosphatase. However, exact mechanisms were not ruled out.

ATP is released by mouse cortical astrocytes that use ATP as an extracellular messenger for calcium wave propagation (Guthrie et al., 1999). Propagating waves of elevated intracellular free calcium were evoked by extracellular electrical or mechanical stimulation of cultured astrocytes. During calcium waves astrocytes released ATP into the medium that evoked calcium responses in adjacent astrocytes. Calcium waves propagated across acellular regions in the absence of any gap

junction communication between astrocytes. These experiments confirmed that ATP was not released from a single point source to diffuse to adjacent astrocytes but was sequentially released by cells along the path of the wave. The excitatory effect of medium samples that were collected from astrocyte cultures during (but not before) calcium wave stimulation and contained ATP were blocked by purinergic receptor antagonists. ATP, applied at the concentrations measured in medium samples, evoked responses that were similar to those evoked by medium samples. Thus the data implicate ATP as a primary active messenger between CNS astrocytes.

In summary, all of these data indicate that in the CNS ATP can be released from neurons during synaptic activity and from astrocytes under electrical stimulation and by activation of glutamate receptors and act as an active messenger in the extracellular communication system of brain cells.

1.11 Release of ATP from Tissues under Different Experimental Conditions.

ATP released into extracellular space is rapidly metabolized by the ecto ATPases and non-specific phosphatases to adenosine. These surface-located enzymes for hydrolysis of ATP have been found along the pre- and post-synaptic membranes and also in glial cell membranes (Sperlagh et al., 1995). The majority of the ATP in the extracellular space is converted to adenosine in less than 1 second (Dunwiddie et al., 1977) which makes it difficult to identify the ATP release. In 1977 White developed a technique for specific detection of ATP using the ATP induced light response of firefly luciferin and luciferase (White, 1977). Using this technique he showed that ATP is released from a synaptosomal preparation during

depolarization induced by increased extracellular K^+ and veratridine (White, 1977; White, 1978). In these experiments the release of ATP was directly and continuously detected by the luciferin-luciferase technique. The released ATP interacted with firefly luciferin and luciferase in the incubation medium to produce light that was detected by a photomultiplier. The studies demonstrated that elevated extracellular K^+ or the depolarizing drug, veratridine, caused release of ATP from a synaptosomal fraction prepared from whole brain. The release of ATP was Ca^{2+} -dependent and had striking similarities with the depolarization-induced release of putative neurotransmitters. The conclusion was made that the ATP was released exocytotically from presynaptic nerve-terminals in the synaptosomal preparation (White and MacDonald, 1990).

The release of ATP from electrically stimulated hippocampal slices has been reported (Wieraszko et al., 1989). Schaffer collaterals of hippocampal slices from rats or mice were stimulated with trains of pulses each of 300 Hz for 50 ms (75 pulses per train) at intervals of 2 seconds. The release of ATP was measured with a luciferase-luciferin system and the produced light was detected by a photomultiplier placed beneath a modified slice chamber. The release of ATP was observed 5-10 seconds after the start of the stimulation. The amount of ATP released from 10 mouse slices and 10 rat slices was 0.55 ± 0.04 pmol/slice and 0.61 ± 0.06 pmol/slice. The electrically evoked release of ATP from hippocampal slices was Ca^{2+} -dependent and was absent in Ca^{2+} -free medium. It was suggested that ATP may be stored and released together with glutamate from activated Schaffer collateral nerve endings.

The data supported the role of ATP as a neurotransmitter or neuromodulator in the CNS.

The Ca^{2+} -dependent release of ATP from rat habenula slices was shown (Sperlagh et al., 1997). ATP and [^3H]ACh were released simultaneously in a significant quantity from the tissue at rest and in response to low frequency electrical field stimulation. Stimulation consisted of square-wave pulses (2.5-ms in duration) applied at 25 V, at 2 Hz for 3 min. The resting release of endogenous ATP was 12.82 ± 0.52 pmol/g/min and the release evoked by electrical field depolarization was 1405 ± 214 pmol/g/min. Perfusion with Ca^{2+} free solution inhibited the evoked-release of ATP and [^3H]ACh as did application of different Ca^{2+} channel antagonists. Therefore the release of the two transmitters was triggered by Ca^{2+} influx through voltage-sensitive Ca^{2+} -channels activated during depolarization. The high correlation between the percent inhibition of ATP release and percent inhibition of ACh release caused by the different Ca^{2+} channel antagonists suggested that a common population of Ca^{2+} channels was responsible for triggering their release but the difference in the time scale of the two neurotransmitters outflow evoked by field stimulation suggested their release from different vesicular compartments.

Endogenous ATP is also co-released with noradrenaline from rat hypothalamic slices (Sperlagh et al., 1998). ATP and [^3H]NA were released simultaneously from the superfused hypothalamic slices in response to electrical depolarization. Electrical field stimulation consisted of square-wave pulses applied at supramaximal voltage with respect to ATP release (25 V) at a frequency between 2 Hz and 16 Hz. The stimulation evoked release of ATP, measured by luciferin-luciferase technique, was

45.2±7.7 pmol/g. Under Ca²⁺-free conditions the stimulation-induced release of ATP and [³H]NA was diminished by more than 80%. Therefore the majority of the release was Ca²⁺-dependent release. The inhibition of the voltage-dependent Na⁺-channel by TTX blocked propagation of the action potential and almost totally abolished the evoked release of ATP. The release of [³H]NA was reduced to a lesser extent. The results supported the view that ATP is involved in the neurotransmission in the hypothalamus, but the source of the released ATP and noradrenaline seemed to be not identical.

ATP can also be released from cellular sites that apparently lack vesicular storage organelles. That ATP is released from cellular systems under conditions of hypoxia has been known for long time. The release of adenine nucleotides, including ATP, from the isolated perfused guinea pig heart was measured under normoxic and hypoxic conditions (Borst and Shrader, 1991). Hypoxic perfusion caused a threefold increase in ATP release amounting to 2-4% of total release of adenine nucleotides. In this case, the release of ATP might be by a carrier or channel similar to the product of the multidrug-resistance gene, P-glycoprotein, that has been implicated as an ATP channel (Abraham et al., 1993).

Investigations were undertaken to measure the release of adenosine and adenine nucleotides, including ATP, from the in vivo normoxic rat cerebral cortex as well as during hypoxic episodes (Phillips et al., 1993). An inhibitor of non-specific phosphatases, DL- α -glycerophosphate was included in artificial CSF used to superfuse the cerebral cortices. Quantitative determination of adenosine and adenine nucleotides in the perfusates was by HPLC techniques (Phillips et al., 1987). The

basal (normoxic) levels of ATP and adenosine were 17.7 ± 2.1 nM and 38.9 ± 10.9 nM correspondingly. During 10 min episodes of hypoxia (8% oxygen inhalation) adenosine levels in the cortical superfusates were doubled, but release of ATP was unaltered. The observations confirmed that ATP is continuously released from the normoxic cerebral cortex, but adenine nucleotide levels are not elevated during hypoxia.

The lack of an effect of hypoxia on ATP release by CNS tissue stands in contrast to the increases in release from hypoxic or ischemic heart. In fact, release of ATP by CNS tissue during injury and the role ATP as an active messenger in extracellular communication system of brain cells in CNS pathology has never been demonstrated (Walz, 1997).

1.12 Rationale and Objectives for Present Investigation.

As discussed above, after focal ischemia, the cells in the core region of ischemia die rapidly. However, in the penumbra located around this ischemic focus the cells are metabolically compromised but not dead. It takes 2 to 3 days for the cells to die after reperfusion of the penumbra. The cells in this region are salvageable. Therapeutic approaches directed toward the treatment of stroke have focused on the salvage of as many of these cells as possible. Microglia, as resident brain macrophages, respond to ischemic cell damage and become activated (Schroeter et al., 1999). Activated microglia are able to synthesize a variety of neurotoxic factors such as reactive oxygen and nitrogen intermediates, proteolytic enzymes, arachidonic acid metabolites and proinflammatory cytokines (Banati et al.,

1993) as well as neurotrophic factors. Therefore microglia might play a role in subsequent neuronal loss or rescue after focal ischemia. In this regard, knowledge of the pathways underlying the changes in the morphology and function of activated microglia is very important in order to find ways to suppress or stimulate microglial function.

It is not unreasonable to postulate a role of extracellular ATP in modulation of microglia. Large amounts of ATP are released by cholinergic, adrenergic and purinergic synapses and also by damaged cells. Significant extracellular ATP concentration may be built up under certain conditions in CNS as shown by detection of ATP release from nerve tissues (Ferrari, 1996). Microglia possesses several types of P2 purinoceptors, activation of which causes changes in membrane permeabilities and cytoplasmic Ca^{2+} concentration.

SD waves activate microglia surrounded by healthy tissue. If during SD waves ATP is released into extracellular space, this phenomenon may provide an experimental tool to understand the signaling pathways between neurons, astrocytes and microglia. The release of ATP during SD waves might be evidence that ATP serves as an extracellular signal for transformation of microglia from the resting to activated form.

The goal of this thesis was to determine whether ATP is released during SD wave propagation in hippocampal slices.

2. MATERIALS AND METHODS.

2.1. Rat Hippocampal Slices.

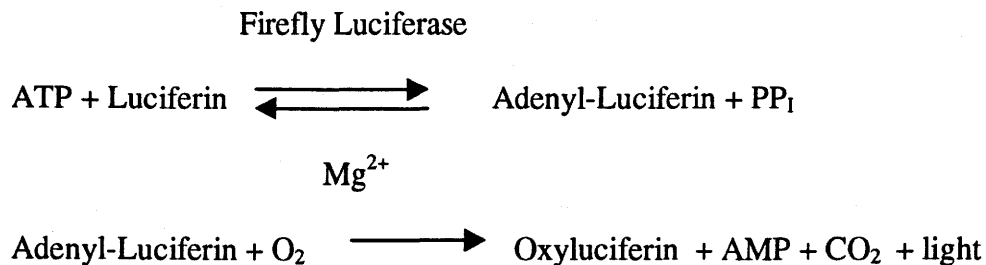
Adult Wistar rats (Charles River Inc., St. Constant, QC, Canada) of 275-350 g (more than 2 months of age) were used in these experiments. The animals were anaesthetized with Methoxyflurane (Janssen Pharmaceutica, Canada) and decapitated. The brains were dissected out and 400 μ m hippocampal slices were cut in frontal orientation on a vibroslicer (Campdem Instruments LTD 752M Vibroslice). In order to provide good viability of the brain tissue the dissections were performed in chilled preparation solution as proposed by Richerson and Messer (1995). Then the slices were washed and stored up to 4 h in artificial cerebral spinal fluid (ACSF) at room temperature before being placed into the experimental chamber. The perfusate samples for measuring ATP content were taken after 1-1.5 hour perfusion of the slices in the experimental chamber.

2.2. Assay of ATP.

2.2.1. Luciferin-luciferase system.

The ATP released from the hippocampal slices was assayed using the luciferin-luciferase technique. The luciferase-luciferin system is the most sensitive system to measure low concentrations of ATP in the solutions. The firefly enzyme luciferase catalyzes the ATP-dependent oxidation of luciferin. This reaction involves the adenylation of a luciferin-luciferase complex with the formation of

pyrophosphate. In the presence of oxygen, this complex decomposes into oxyluciferin, adenosine monophosphate, carbon dioxide and luciferase.



ATP is consumed and light is emitted when firefly luciferase catalyzes the oxidation of luciferin. One photon is released per mole of oxidized luciferin. When ATP is the limiting reagent the light emitted is proportional to the ATP present.

2.2.2 Technical Procedure.

The ATP Bioluminescent Assay Mix (Sigma, USA), containing luciferase, luciferin, MgSO_4 , DTT, EDTA, bovine serum albumin and tricine buffer salts, was employed for the quantitative bioluminescent determination of ATP in the samples. To ensure reproducibility, low background, and maximum sensitivity, the components of the kit were reconstituted in sterile filtered distilled water. All assays vials, glassware and pipet tips coming into contact with any of the samples or reagents were as clean and as free from ATP and bacterial contamination as possible. Pipet tips were never used for more than one transfer and were not allowed to come into contact with skin or other contaminating surfaces before use. The

solutions of ATP Assay Mix were stable for two weeks if stored at 0-5°C and protected from light. Because a slight decrease in light production and sensitivity may occur during this time a new standard curve was prepared each day before use. The standard calibration curve was prepared from different concentrations of ATP ranging from 2×10^{-9} to 10^{-12} M.

2.2.3 Luminescence Measurements.

The luminescence was measured in a luminometer Lumat LB 9501 (EG and G Berthold). The quantity of light measured over a 30-second selected measuring time was output in Relative Light Units (RLU) for each sample. The measurement mode allowed one automatic 100 µl injection of ATP Assay Mix solution per 100 µl sample and immediately followed by measurement of light emission. For each sample the amount of background (BG) light produced was measured and subtracted from that obtained for the sample after injection of ATP Assay Mix solution. This final value expressed in RLU per second was proportional to the amount of ATP in the sample.

2.3 Electrophysiological Setup.

2.3.1 SD Recording.

For electrophysiological recordings, hippocampal slices were isolated and placed in a perfusion chamber. The chamber was continuously perfused with

oxygenated ACSF. The recording electrode was positioned in stratum radiatum of the CA1 region of the hippocampal slice. The extracellular potential was amplified with the Axonprobe-1A Microelectrode Amplifier (Axon Instruments, Inc., USA) and recorded with an ink recorder (Gould Inc., USA). Recording glass capillary electrodes were made of borosilicate capillaries (Hilgenberg, Germany) with a 1.5 mm outer diameter, 0.26mm wall thickness, a tip diameter of not more than 20 μm and filled with ACSF. The “ground” electrode was placed into the external solution.

2.3.2 SD Triggering.

SD waves were triggered by means of a glass micropipette with its tip broken back to a diameter of $\sim 5\ \mu\text{m}$, filled with 1.2 M KCl, connected to the A203 Nanoliter Injector (World Precision Instruments, Inc., USA). The glass capillary tip was positioned in stratum radiatum of the CA1 region of the hippocampal slice approximately 1.0 mm distant from the recording electrode. 73.6 nl of 1.2 M KCl injected into the slice reliably evoked an SD wave that was recorded with extracellular recording electrode.

In the other experiments SD waves were triggered by application of 100 μM ouabain in the perfusion fluid. After the chamber with the slice was perfused with ACSF for 1-1.5 hour, ouabain was applied. The evoked SD wave was monitored with the extracellular electrode positioned in the stratum radiatum of the CA1 region of the hippocampal slice.

2.3.3 Brain Slice Chambers and ATP Sampling.

Three kinds of the brain slice chambers were used in the experiments. In the first series of experiments six brain slices were placed in the BSC-ZT submersion chamber (chamber 1) (Medical System Corp., USA) in which brain slices were supported on a stiff nylon mesh to allow the perfusion solution to flow transversely across both cut surfaces. The chamber had a volume of 0.7ml and was perfused at a rate of 1ml/min using a peristaltic pump (LKB BROMMA, Sweden). In all series of experiments after 1-1.5 hour superfusion period to equilibrate the tissue, samples were collected, and assayed for ATP.

In the second series of the experiments one slice was placed in a glass bottom chamber with a volume of a 0.3ml (chamber 2). The slice was held by covering it with piece of fine nylon that was weighted with U-shaped metal clip made from platinum. The perfusion solution flow transversely across one cut surface and outflow was provided by a vacuum pump (Cole-Parmer Instrument Co., USA). The chamber was perfused at a rate of 1ml/min.

In the third series of experiments one slice was placed into a 0.3ml volume chamber (chamber 3grav.) by the same manner as it was in the second series of experiments. The perfusate outflow was provided by gravity force. The flow rate of the solution was 1 ml/min.

In the fourth series of experiments two chambers were used: a 0.3ml volume (chamber 3grav.) and a 0.15ml volume (chamber 4vac.). The chambers were perfused at a rate of 1 ml/min provided with gravity force or with vacuum pump (Cole-Parmer Instrument Co., USA), respectively.

2.4 Lyophilization of Samples.

The ATP standards were frozen (-50 - -70°C) and lyophilized in a Freeze Dry-3 (Labconco) lyophilizer under a vacuum, sublimating the ice into water vapour. The dry standards were reconstituted in the sterile filtered distilled water at 10 times less volume and standard curve was prepared.

2.5 Experimental Protocols and Solutions.

2.5.1 SD in the Hippocampal Brain Slices.

In the first series of experiments the SD waves were evoked by changing normal ACSF to ACSF containing 100 μM ouabain. In these experiments SD waves were not recorded with extracellular electrode. Six hippocampal slices were placed in the chamber 1 and perfused continuously with oxygenated ACSF for 1-1.5 hour. Then 1min perfusate samples were collected before and during application of ouabain. The basal outflow was taken to be the outflow in the 6 min before switching the solutions. The overflow of ATP induced by ouabain was calculated by subtraction of the basal outflow from the total outflow of ATP measured in the 25 min after addition of ouabain. As in any experiment the perfusate samples were collected into microvials and inserted into a container of ice chips and stored for 3-4 hours until assayed for ATP. All solutions used in the experiments were sterile filtered to avoid bacterial contamination. A standard calibration curve was prepared from the standards with known concentration of ATP ranging from $1.8 \times 10^{-9}\text{M}$ to $3.5 \times 10^{-12}\text{M}$ (see Fig 2.1) every time before testing the perfusate samples.

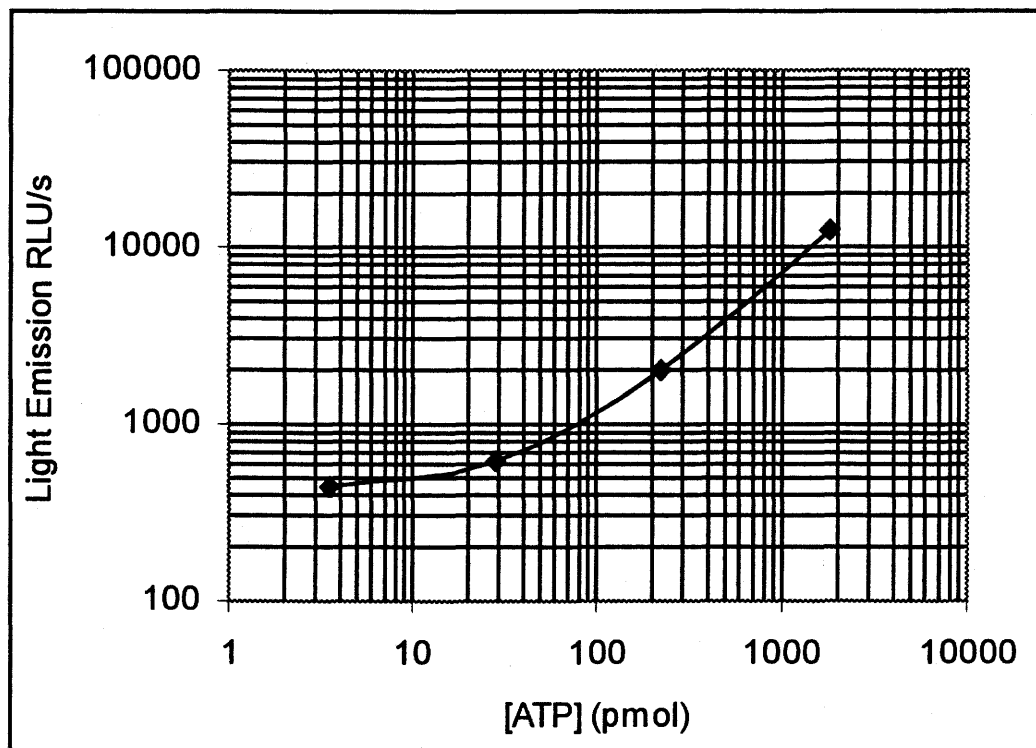


Fig.2.1 Typical ATP calibration curve. The ATP standards were prepared in sterile filtered ACSF and contained different concentrations of ATP ranging from 1.8×10^{-9} to 3.5×10^{-12} mol. The light emission was measured by luminometer over a 30-second period following addition of ATP Assay Mix solution to the ATP standard and expressed in Relative Light Units per second (RLU/s). Each point is a mean of 2-3 measurements of the standards containing the same amount of ATP.

In the second series of experiments one hippocampal slice was placed into the chamber 2 and the extracellular recording electrode was positioned in the CA1 region of the hippocampal slice. The amplified extracellular potential was monitored by ink recorder before and after application of ouabain. A delay in an appearance of SD wave following switching from normal ACSF to a medium containing ouabain, the duration and an amplitude of the SD wave were recorded and analyzed.

In the third series of experiments the hippocampal slice was placed into the chamber 3grav. For each experiment the recording electrode and a glass capillary tip of the Nanoliter Injector filled with 1.2M KCl were positioned approximately 1mm apart in stratum radiatum of the CA1 region. SD wave was triggered by injection of KCl into the slice. SD wave was monitored by ink recorder and 30-s perfusate samples were collected before triggering of SD wave, during SD wave and during the recovery period.

2.5.2 ATP Dilution in the Slice Chambers.

In the fourth series of experiments 4.6 and 46 nl of 1mM ATP were injected with the Nanoliter Injector into the experimental chamber 3grav. and the chamber 4vac. where a slice was not placed, but all experimental conditions were imitated. (The perfusate flowed at a rate of 1ml/min. The U-shape metal clip placed on the chamber bottom, a glass micropipette tip of Nanoliter Injector was submerged at the same depth as the surface of the slice during the experiment.) 30-s samples were collected continuously before, during and after injection of ATP into the chamber.

2.5.3 Hydrolysis of ATP by Ectonucleotidases and Non-specific Phosphatases in the Slice.

147.2 nl of 100 μ M ATP was injected into the hippocampal slice placed into the chamber 4vac. and into the same chamber without the slice. The tip of a glass micropipette of the Nanoliter Injector was plunged into the hippocampal slice tissue at approximately a 200 μ m depth. At the same depth and position the tip of a micropipette was placed during ATP injection into the chamber without the slice. Perfusate was collected every 30 s before, during and after injection of ATP. The flow rate of the perfusate was 1ml/min.

2.5.4 Solutions.

The hippocampal rat brain slices were perfused with ACSF contained 125.5 mM NaCl, 3.5 mM KCl, 2 mM MgSO_4 , 2 mM CaCl_2 , 10 mM glucose, 26 mM NaHCO_3 , and bubbled with 5% CO_2 /95% O_2 . The preparation solution was the same except it was Ca^{2+} -free and included additionally 200 mM sucrose and 1mM kynurenic acid (Sigma) (Richerson and Messer, 1995). For triggering SD by ouabain ACSF containing 100 μ M ouabain (Sigma) was used. The extracellular recording electrode was filled with ACSF. The glass micropipette of the Nanoliter Injector was filled with 1.2 M KCl.

For the determination of ATP concentration in the samples an ATP Bioluminescent Assay Kit was employed (Sigma). The contents of one vial of ATP Assay Mix was dissolved in 5ml of sterile water to generate a stock solution with pH of 7.8. The luminometer equipped with a fast mixing device allowed rapid addition

of 0.1ml of ATP Assay Mix solution to 0.1 ml of standard or sample in reaction vial and analysis of the light emission in the seconds which followed the mixing.

A similar ATP assay prepared in the laboratory was used in the experiments as well. It contained firefly luciferase 0.33 mg (L-9506, Sigma), luciferin 0.83 mg (L-6882, Sigma), MgSO_4 6 mg, EDTA 2 mg, DTT 0.08 mg, bovine serum albumin 5 mg, Tricine 45 mg, reconstituted in 5ml sterile water (Sperlagh et al., 1998).

The ATP standards for the standard calibration curves were prepared in sterile filtered ACSF and contained different concentrations of ATP ranging from 1.8×10^{-9} to 1.4×10^{-11} or 3.5×10^{-12} M. In the series of experiments with DMSO the chemical was added to the standards in the proportions 1%, 5%, and 10% of their volume. In the group of experiments for determination of luciferin-luciferase complex activity in the solutions containing different drugs, the drugs were dissolved in the ATP standard medium. All general chemicals were supplied by Sigma (St. Louis, MO). Ouabain was purchased from Boehringer Mannheim Biochemica (Germany).

2.6 Data Analysis.

The kinetics of firefly luciferase light emission are characterized by a flash period lasting a few seconds followed by a period of lower intensity light emission which extends over minutes. The luminometer Lumat LB 9501 allowed integration of the photons emitted through the first 30-second period which followed the mixing of reagents. The light emission of the samples and ATP standards was measured in RLU. The amount of background light produced by each sample or ATP standard was measured before reagent mixing and was subtracted from the value that

obtained after mixing. This final value expressed in RLU/s was proportional to the amount of ATP in the sample or ATP standard. The ATP levels in the samples were calculated by double log curve fitting program and expressed in nmol.

Since enzymatic activity of luciferase-luciferin system is different in normal ACSF and the ASCF containing drugs, separate ATP calibration curves were prepared on the basis of these solutions to estimate ATP concentrations under different experimental conditions.

2.7 Statistical Methods.

Results are given as means \pm S.E.M. from n observations. Differences between means were tested for significance by Student's t-test. A P-value less than 0.05 was taken to be statistically significant.

3. RESULTS

3.1 ATP Release Caused by Application of Ouabain to six hippocampal slices.

The basal outflow of ATP from six slices placed into the chamber 1 in the 6 min before addition of ouabain averaged 3.3 ± 1.6 pmol/slice/min (n=3). Ouabain elicited a transient overflow of ATP 10.4 ± 4.4 pmol/slice/min at the concentration 100 μ M (Fig.3.1). Ouabain caused the significant increase in the ATP release ($P<0.05$) from the rat hippocampal slices. The maximal increase of the outflow of ATP was 4-fold. The increase in ATP outflow started with the delay 3.7 ± 1.2 min after application of ouabain and had a duration 7.1 ± 3.9 min.

3.2 SD Waves Caused by Application of Ouabain.

One slice was placed into the chamber 2. Application of 100 μ M ouabain triggered SD waves (Fig.3.2) with an amplitude of 6.5 ± 5.2 mV (n=19) and duration of 11.4 ± 5.2 min (n=19). SD waves appear with 7.5 ± 2.8 min delay after the beginning of the incubation of the slice in the perfusate containing 100 μ M ouabain.

3.3 ATP Release from a Single Slice.

The basal outflow of ATP from the single slice placed into the chamber 3grav. after 1-1.5 h of adaptation period was not possible to determine because the concentration of ATP in the collected samples was below 10 pmol. In this range of

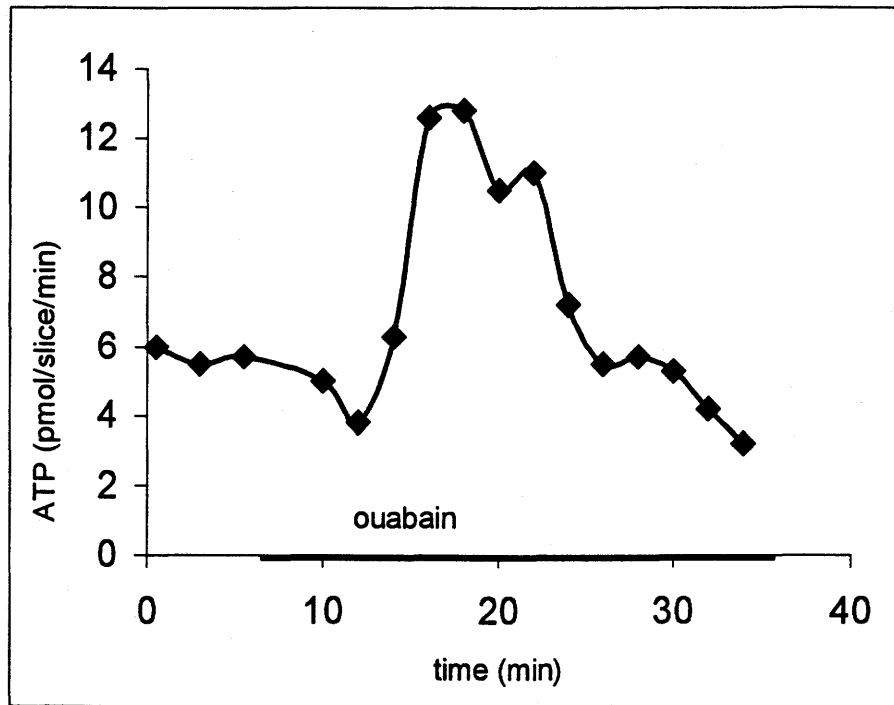


Fig.3.1 Ouabain triggered ATP release from rat hippocampal slice. Representative example of resting and ouabain-evoked release of ATP from the isolated 400 μm rat hippocampal slice. SD wave was artificially elicited in six slices by application of 100 μmol ouabain into the perfusion fluid. The slices were superfused at a rate of 1 ml/min. 1 min samples were collected and assayed for ATP with ATP Bioluminescent Assay Kit (Sigma) before and during application of ouabain. ATP release expressed in pmol/slice/min.

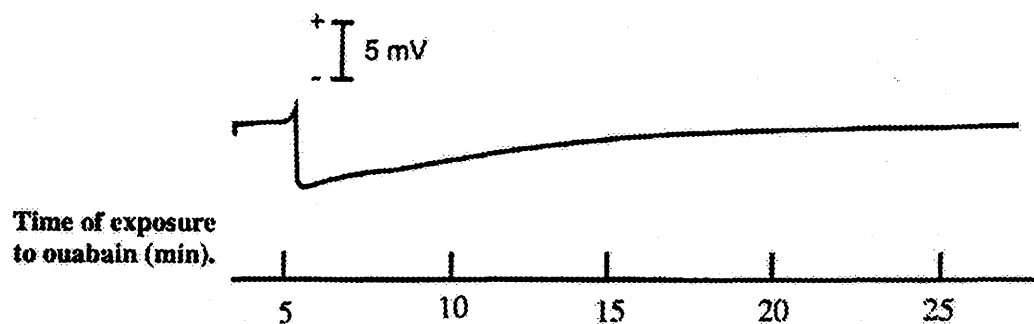


Fig.3.2 *SD wave triggered by application of ouabain.* SD wave was triggered by application of 100 μmol ouabain into perfusion medium. The evoked SD wave was monitored with the extracellular electrode positioned in the stratum radiatum of the CA1 region of a 400 μm rat hippocampal slice. Ouabain triggered SD waves with the amplitude 6.5 ± 5.2 mV ($n=19$) and the duration 11.4 ± 5.2 min that appeared with the 7.5 ± 2.8 min delay after switching normal ACSF to ACSF containing ouabain.

ATP concentrations the amount of light produced by luciferase-luciferin system is close to background light emission. In this range, the amount of light is not proportional to the amount of ATP in the standards or samples, thus making determination of ATP concentrations impossible.

SD waves evoked by application of KCl (Fig.3.3) did not raise the ATP concentration in the perfusate enough to be detected by luciferin-luciferase system (n=3). The concentration of ATP in the 30-second samples collected during SD wave and recovery period was still below $1.0 \times 10^{-11} \text{M}$.

3.4 Attempts to Decrease ATP Dilution in the Slice Chamber.

In order to determine how quickly released ATP would be washed out of the chamber or how much it would be diluted, 4.6 nl and 46 nl of 1 mM ATP were injected in two different chambers without slices. For the 0.3 ml chamber (chamber 3grav.) with the outflow provided by gravity force ATP was detected in 6-7 30-second and 0.5 ml samples after injection (Fig.3.4). The same amounts of ATP injected in the 0.15 ml chamber (chamber 4vac.) with outflow provided with a vacuum pump ATP was detected in 2-3 samples after injection (Fig.3.5). It means that ATP was diluted 2-3 times less in the smaller chamber with a vacuum pump than in bigger one.

Experiments for detection of ATP release from a single slice using the chamber 0.15 ml (chamber 4vac.) with outflow provided with the vacuum pump

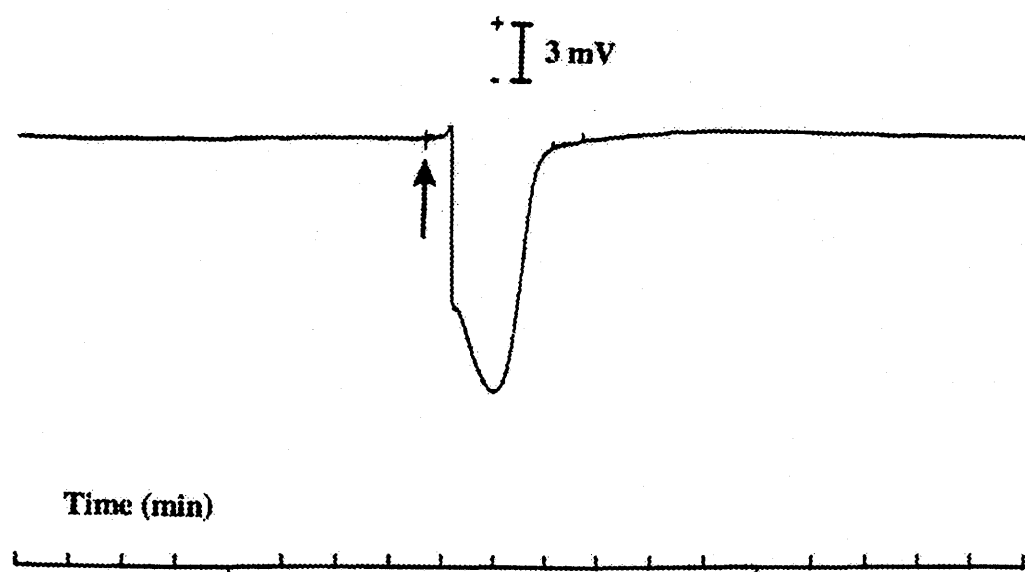


Fig.3.3 *SD wave triggered by high potassium.* SD wave was triggered by means of a glass micropipette with its tip $5\mu\text{m}$ (outer diameter) filled in with 1.2 M KCl. 73.6 nl of KCl reliably evoke SD waves in rat hippocampal slices. Evoked potential was recorded with extracellular electrode inserted in stratum radiatum approximately 1 mm apart of the injection electrode.

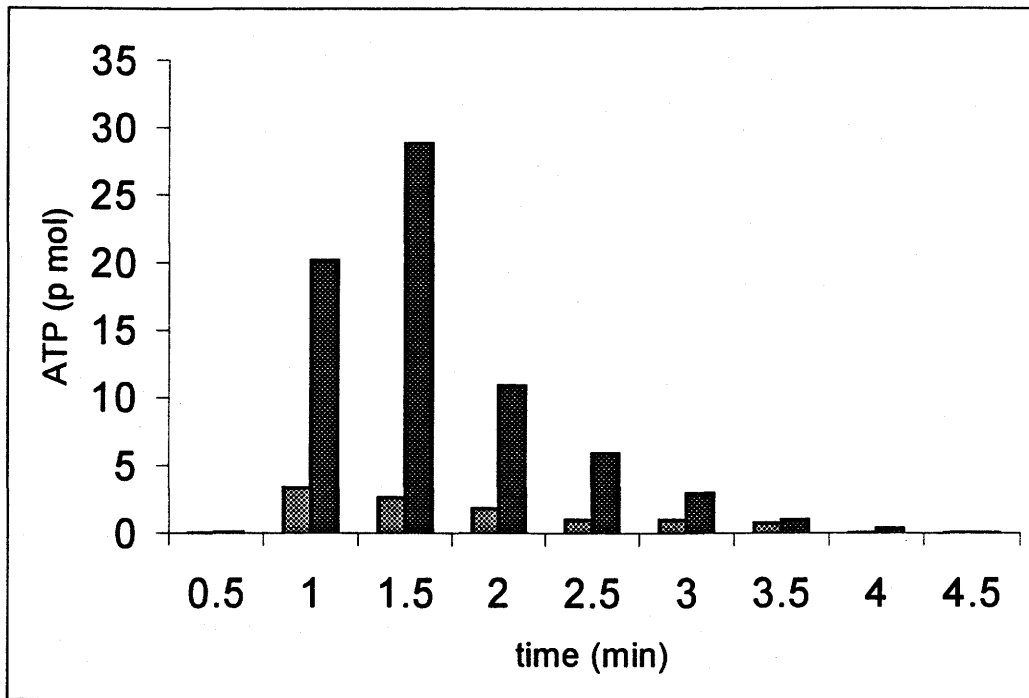


Fig.3.4 *ATP dilution in the chamber of 0.3 ml volume and outflow provided by gravity force. 4.6 nl and 46 nl of 1 mM ATP were injected into the chamber. Amounts of ATP in 30-s samples collected before and after injection shown by gray (4.6 nl injected) and dark (46 nl injected) bars. ATP was detected in 6-7 30-s samples after injection. ATP was injected in the beginning of the collection of the second sample. The perfusate flow rate was 1 ml/min.*

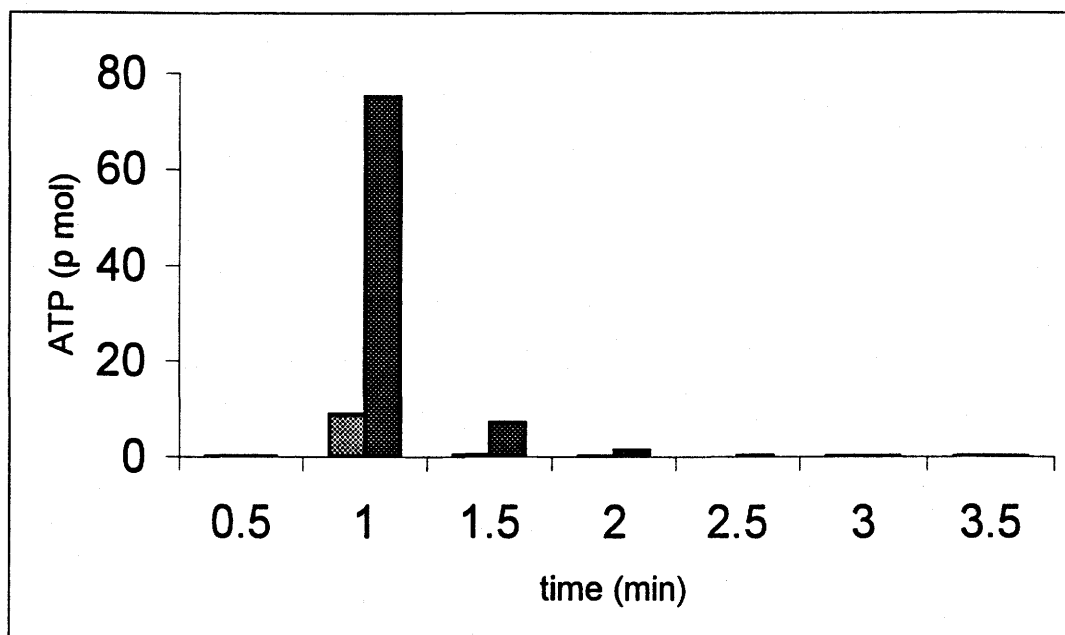


Fig.3.5 *ATP dilution in the chamber of 0.15 ml volume and outflow provided by a vacuum pump. 4.6 nl and 46 nl of 1 mM ATP were injected into the chamber. Amounts of ATP in 30-s samples collected before and after injection shown by gray (4.6 nl injected) and dark (46 nl injected) bars. ATP was detected in 2-3 30-s samples after injection. ATP was injected in the beginning of the collection of the second sample. The perfusate flow rate was 1 ml/min.*

were not successful: the amounts of basal ATP release and its release during and after SD wave elicited by KCl were below the limit of detection (n=9).

3.5 Hydrolysis of ATP by Ectonucleotidases and Non-specific Phosphatases in Rat Hippocampal Slice.

The ability of ectonucleotidases and non-specific phosphatases to hydrolyze extracellular ATP was evaluated by injection of 147.2 nl of 100 μ M ATP into the hippocampal slice and in the chamber in 5-10 min after the slice was taken out (Fig.3.6). The maximum of ATP concentration detected in 30-second samples after ATP injection into the slice and empty chamber were 11.2 ± 2.7 nmol and 31.7 ± 3.3 nmol respectively (n=4). Therefore, ectonucleotidases and non-specific phosphatases located on the neuronal and glial cell membranes hydrolyzed approximately 2/3 of ATP injected in extracellular space.

3.6 Interference of Blockers of Ectonucleotidases and Non-specific Phosphatases with Luciferin-luciferase System.

Inclusion of an effective inhibitor of ecto 5'-nucleotidase α,β -methylene-ADP (50 μ M) and an inhibitor of non-specific phosphatases DL- α -glycerophosphate in ATP standard medium led to the increase of the light emission (Fig.3.7). The standard curve prepared for standards containing the drugs had a smaller slope. Therefore a strong correlation between the light produced and ATP concentration in the standards was lost which made it impossible to determine ATP concentration in

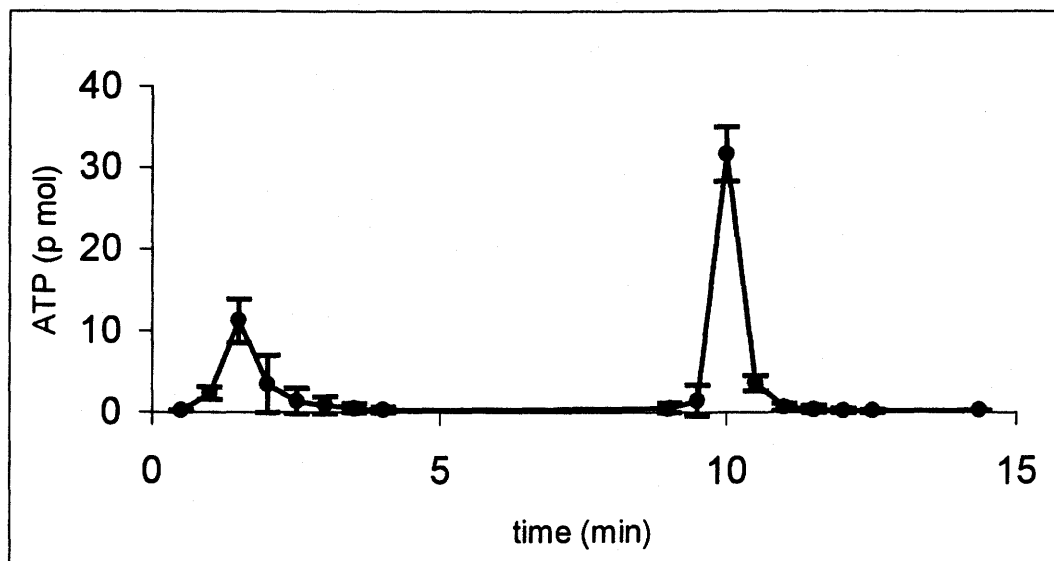


Fig.3.6 *Hydrolysis of extracellular ATP by ectonucleotidases and non-specific phosphatases.* ATP (147.2 nl, 100 μ M) was injected into the 400 μ m rat hippocampal slice and in several minutes later, after the slice was taken out, into the empty chamber with running perfusate. 30-s perfusate samples were collected continuously before, during and after injection. ATP was injected into the slice during collection of the second sample. The maximum amounts of ATP detected in the perfusate samples after injection into the slice and the empty chamber were 11.2 ± 2.7 pmol and 31.7 ± 3.3 pmol respectively ($n=4$). Approximately 2/3 of ATP injected into the extracellular space was hydrolysed by ectonucleotidases and non-specific phosphatases.

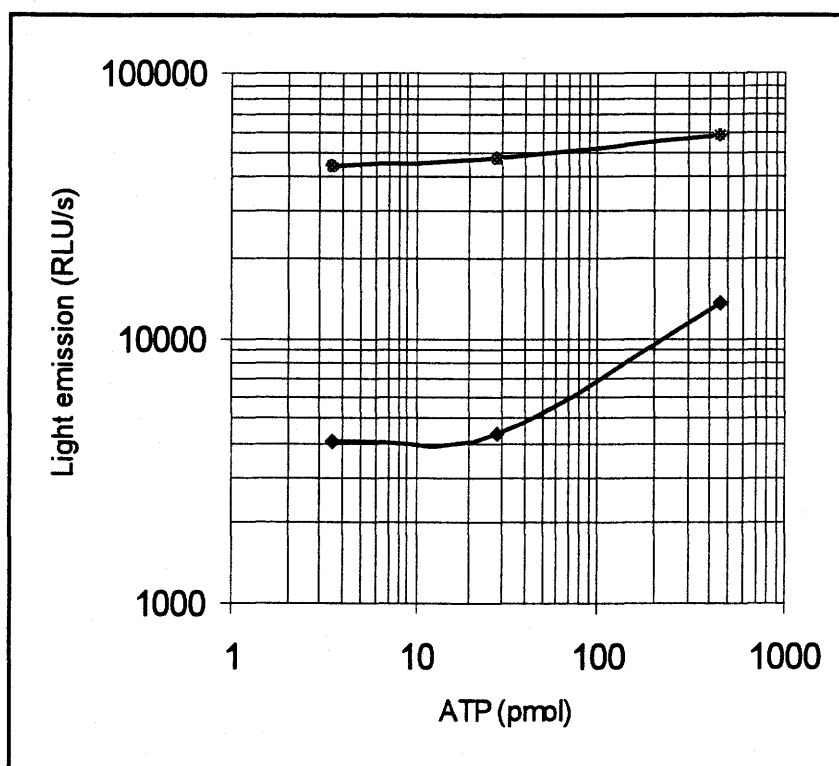


Fig.3.7 *ATP calibration curves prepared with the ATP standard solutions of different content.* ATP calibration curve prepared for standards without drugs added (♦) and ATP calibration curve for standards including an inhibitor of non-specific phosphatases DL- α -glycerophosphate (5 mM) and an inhibitor of ectonucleotidases α,β -methylene ADP (50 μ M) (●). Inclusion of the drugs in the ATP standard media increased light emission and decreased sensitivity of luciferin-luciferase system. Strong correlation between light emitted and ATP concentration in the standards was lost.

the samples containing these two drugs in the medium. Presence of α,β -methylene-ADP and DL- α -glycerophosphate in the ACSF led to decrease of luciferin-luciferase system sensitivity.

3.7 Lyophilization of Samples.

The standards with different concentration of ATP ranging from 1.4×10^{-11} M to 1.75×10^{-12} M were concentrated 10-fold by lyophilization and standard curves were prepared (Fig.3.8). The light intensity dropped sharply in the condensed standards indicating the loss of luciferase activity in the solution of higher ionic strength. The chemiluminescence intensity was approximately the same for different ATP concentrations which made it impossible to define concentration of ATP in the condensed samples using this calibration curve.

3.8 Effect of DMSO on Sensitivity of Luciferin-luciferase System.

DMSO was added to ATP standards in different proportions: 1%, 5% and 10% of the standard volume. Inclusion of DMSO in ATP standards did not change the sensitivity of luciferin-luciferase system but made the light emission unstable: it was not possible to define the concentration of ATP in the samples. The light emission was not proportional to the ATP concentrations in the samples or in the standards (Fig.3.9).

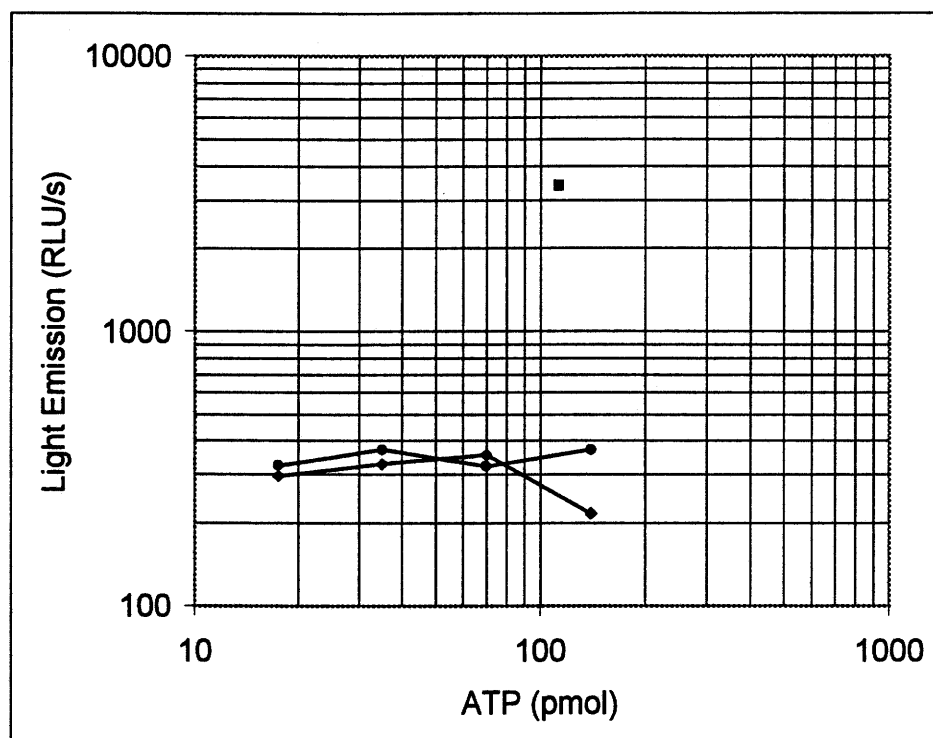


Fig.3.8 *ATP calibration curves prepared for standards concentrated 10-fold.* Standard calibration curves were prepared for standards concentrated 10-fold (\diamond , \bullet). The increase of ionic strength of the solutions led to the sharp decrease in luciferase activity and chemiluminescence intensity. Sensitivity of luciferin-luciferase system was lost making it impossible to determine the concentration of ATP in concentrated samples. Point (\blacksquare) shows the light intensity for non-condensed standard with ATP concentration 110 pmol.

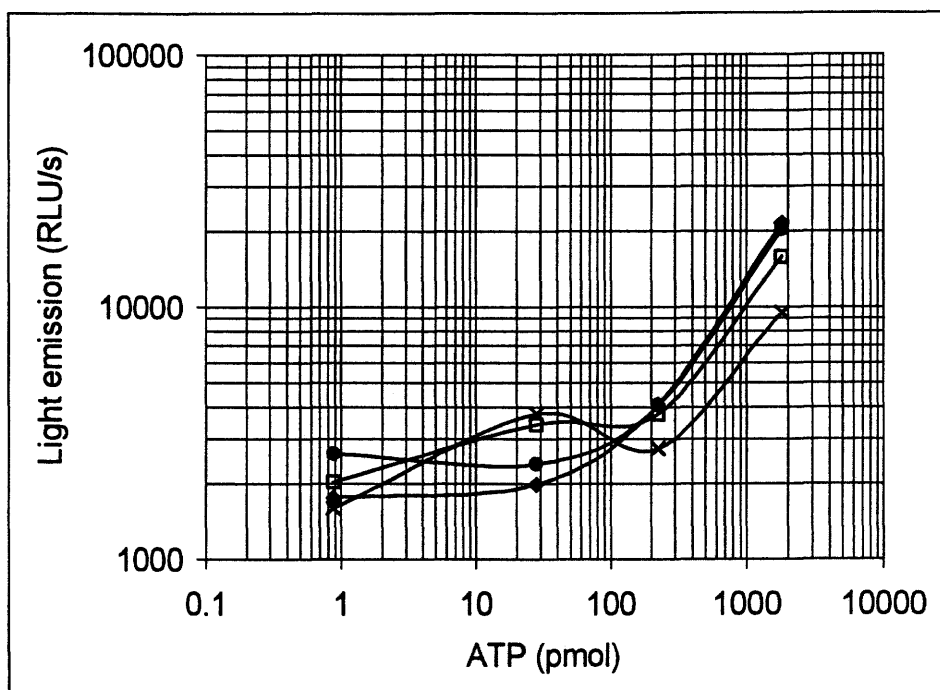


Fig.3.9 *ATP calibration curves prepared for standards containing DMSO.* DMSO was added to ATP standard solution in different proportions: 1% (●), 5% (□), 10% (×). ATP calibration curve for standards without DMSO added (♦). Inclusion of DMSO in the ATP standard media did not change the sensitivity of luciferin-luciferase system but made chemiluminescence intensity unstable. Light emission was not proportional to ATP content in the standards.

3.9 Luciferase Chemiluminescence and the Enzyme Concentration.

The final luciferase concentration in the reaction medium was increased from 0.024 mg/ml to 0.047 mg/ml. This did not increase the sensitivity of the assay although it enhanced the light emission (Fig.3.10).

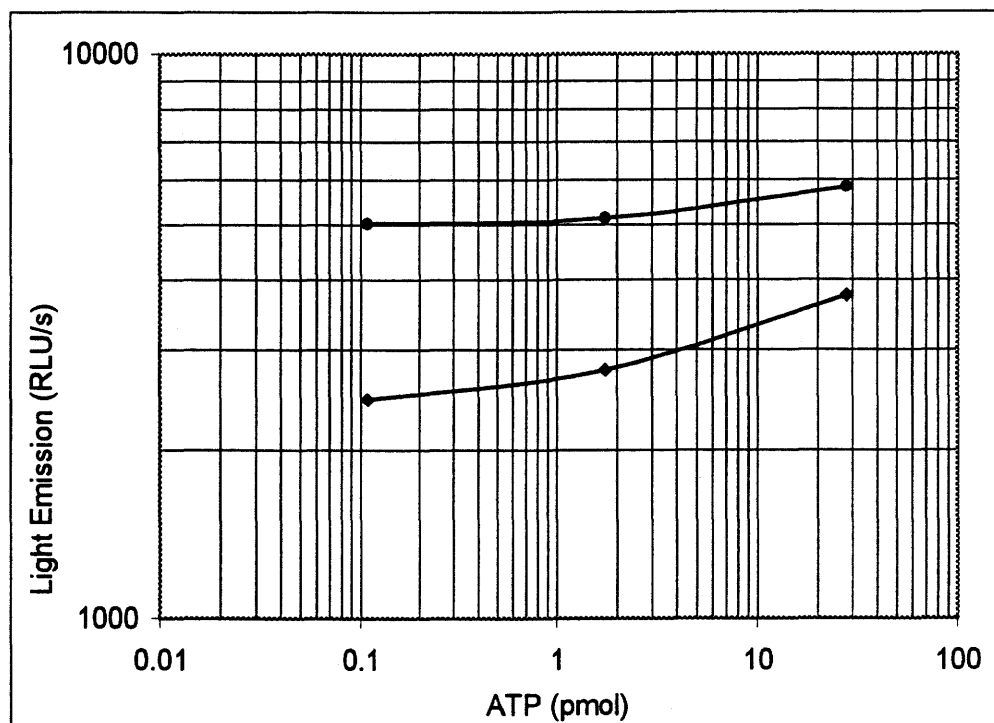


Fig.3.10 *Effect of luciferase concentration on the light emission and sensitivity of the assay.* Concentration of luciferase in the reaction medium was increased from 0.024 mg/ml (♦) to 0.047 mg/ml (●). The increase of luciferase concentration resulted in higher luminescence intensity and almost unchanged sensitivity of the assay.

4. DISCUSSION

4.1 Application of Ouabain Causes ATP Release.

The results obtained in the experiments with SD waves elevated by application of ouabain showed a significant transient increase in ATP outflow during the early period of the incubation of the hippocampal slice in the medium containing ouabain. This increase might be caused by SD wave that propagated across the slice. The release of ATP and recording of SD wave were performed in different groups of the experiments. The delay in appearance of SD wave and the transient increase of ATP in the perfusate were significantly different ($p < 0.05$). ATP release happened before the electrical change. The duration of SD wave and the duration of the transient increase of ATP were not significantly different ($p < 0.1$). It is possible that ouabain itself causes ATP release from the hippocampal tissue. Ouabain is a potent, long lasting and selective inhibitor of Na^+/K^+ -ATPase which is a critical enzyme in brain cells for regulation of membrane potential, cell volume and the trans-membrane fluxes of ions and organic molecules that are co-transported with sodium (Stahl, 1984). Transport of Ca^{2+} via the plasma membrane $\text{Na}^+/\text{Ca}^{2+}$ exchanger depends on the Na^+ electrochemical gradient and small alterations of $[\text{Na}^+]_i$ may influence $[\text{Ca}^{2+}]_i$. Inhibition of Na^+/K^+ -ATPase activity may cause depolarization, cell swelling and the increase in the intracellular concentrations of sodium and calcium which are potentially toxic for the cells (Lees, 1991). The findings demonstrated that a low dose 0.1 nmol of ouabain produced, in vivo, a neuron-selective lesion in the rat hippocampus, although intrahippocampal injection of a higher dose 1nmol of

ouabain produced infarction and non-selective lesions (Lees et al., 1990; Lees and Leong, 1994).

The Na⁺ pump catalytic subunit α has three isoforms $\alpha 1$, $\alpha 2$, and $\alpha 3$ that are expressed in rat hippocampal neurons, and $\alpha 1$ and $\alpha 2$ expressed in glia. These three isoforms differ in their affinities for ouabain: $\alpha 2$ and $\alpha 3$ have high affinities for ouabain, while $\alpha 1$ has a low affinity for ouabain (Sweadner, 1989). The doses 1-10 μM of ouabain, which inhibit $\alpha 2$ and $\alpha 3$ isoforms but negligibly effect $\alpha 1$ in the rat, altered the spontaneous $[\text{Ca}^{2+}]_i$ oscillations and waves in co-cultures of rat hippocampal neurons and glia. The dose $\geq 100 \mu\text{M}$ of ouabain completely inhibits all Na⁺ pump isoforms and causes sustained increases in neuronal $[\text{Ca}^{2+}]_i$ and transient $[\text{Ca}^{2+}]_i$ increases in glial cells. This dose is also associated with increased $[\text{Na}^+]_i$ and $[\text{H}^+]_i$ in neurons and glia (Monteith and Blaustein, 1998). It was shown that ouabain induced nuclear condensation and DNA fragmentation. The doses 10-100 μM of ouabain are neurotoxic and induce a Na⁺-dependent elevation of $[\text{Ca}^{2+}]_i$ (Mark et al., 1995). Although in these experiments the minimum time of exposure to ouabain that was checked for the changes in extracellular ion concentrations was 10-15 min (Monteith and Blaustein, 1998) while for neurotoxicity of the inhibitor 3 hours were required (Mark et al., 1995). However, we can not reject the possibility that in our experiments ouabain caused neuronal damage and leak of ATP into extracellular space. Indeed, it was impossible to evoke the second SD wave in the same slice after washing out the inhibitor which indicated damaged tissue. Therefore application of 100 μM ouabain to elevate SD wave in the hippocampal rat slice by

itself might cause tissue damage and release of ATP into the perfusate that was detected in our experiments.

4.2 Attempts to Measure ATP Release from a Single Slice.

The release of ATP during SD wave evoked by ouabain can not be considered definitive evidence that SD wave cause ATP release from nerve tissue because the inhibitor not only triggers SD wave but also is able to damage brain cells causing osmolysis and calcium necrosis (Lees, 1991). In the next series of experiments we attempted to detect ATP release during SD wave elevated by local injection of high KCl into the hippocampal slice. To find out a correlation between possible release of ATP and SD wave propagation, the extracellular potential was monitored simultaneously with the collection of the perfusate samples. In these experiments we faced the problem that the amount of ATP released from the slice into the perfusate was not high enough to be measured with the luciferase-luciferin system. To solve this problem the smaller chamber was designed that allowed 2-3 time less dilution of ATP. This was still not sufficient for a measurement. The final concentration of ATP in the extracellular space results from a balance between the amount of ATP released and the rate of ATP hydrolysis by a chain of ecto enzymes, non-specific phosphatases and ectonucleotidases. Our data with comparison of ATP injected into the rat hippocampal slice and in the empty chamber demonstrated that approximately 2/3 of extracellular ATP amounts are hydrolyzed by ecto enzymes. The use of the inhibitors of these enzymes was unworkable because the drugs

interfered with luciferase and luciferin, increasing the light emission and lower the sensitivity of the assay.

Concentration of the perfusate samples 10-fold by lyophilization increased the salt concentration in the samples and this in turn had an inhibitory effect on luciferase and decreased the light emission and sensitivity of the system. It is known that the structure of the enzyme, the binding of the substrates and products may be influenced by general ionic strength effects as well as by specific anions or cations. It was shown previously that the activity of firefly luciferase was very sensitive to the presence of salts in the reaction medium (Denburg and Elroy, 1970; Gilles et al., 1976). It appeared that general ionic strength effected the binding between luciferase and ATP. When the ionic strength was increased the interaction between enzyme and ATP was decreased resulting in inhibition of the reaction catalyzed by luciferase and decrease of the light production. It was assumed that a small localized conformational change was occurring in the area of the active site upon the binding of the anions (Denburg and Elroy, 1970) which was responsible for modification in "luciferin-luciferase" activity (Gilles et al., 1976). In our experiments the increase of the salt concentration in the samples 10-fold almost completely inhibited light emission produced by luciferin-luciferase system. The light produced did not differ for the samples with different concentration of ATP thus sensitivity of the system was lost.

We tried to increase luciferase concentration to determine how increased concentration of the enzyme effected the light emission of luciferin-luciferase system. The intensity of the light emission was previously reported to be

proportional to the enzyme concentration (Wet et al., 1987). Our data showed that the increase of luciferase concentration two-fold enhanced intensity of the light emission. For our purposes the most important effect of increased enzyme concentration was on the sensitivity of luciferin-luciferase system that was not previously investigated. We found out that the sensitivity did not change with the increase of luciferase concentration in the reaction medium. We checked the ability of DMSO to increase sensitivity of luciferin-luciferase system (Dr. D. Chedrese, personal communication). The addition of DMSO in different concentrations into the samples made the light emission unstable and this therefore did not allow us to prepare the calibration curve. Thus, all attempts to measure ATP release from a single hippocampal slice using our technique and methods were not successful.

ATP release from one hippocampal rat slice was detected by Wieraszko et al. (1989). The investigators used a specially designed apparatus that combined a luciferin-luciferase assay system with a modified brain slice chamber. The slice was placed into the 0.8 ml transparent chamber that was mounted over a photomultiplier. Ten minutes before the start of each experiment a solution of luciferin-luciferase was added to the chamber. The slice was not perfused during the experiment. Schaffer collaterals of rat hippocampal slice were electrically stimulated with bursts of pulses and in 5-10 second after the start of the stimulation release of ATP was observed as light emitted from the chamber bottom, and detected by the photomultiplier. To find out the amount of ATP released from one hippocampal slice various ATP concentrations were injected directly into the chamber containing the slice in the luciferin-luciferase solution. The amount of light emitted from the chamber was

proportional to the amount of ATP added, that allowed the preparation of an ATP calibration curve. The amount of ATP released from one hippocampal slice during electrical stimulation was determined using this calibration curve and ATP at a concentration $6.2 \times 10^{-11} \text{M}$ and higher could be detected. This technique was unsuitable for our purposes because the technique would not allow us to measure the basal release of ATP from a single hippocampal slice and would not allow the use of on line sampling over an extended time period. Also the stop of the perfusion in Wieraszko's et al. experiments would have caused an ischemic episode, which would have complicated the analysis in our experiments. With our technique we were able to detect ATP concentrations at $6.2 \times 10^{-11} \text{M}$ but the specific conditions of our experiments required a higher sensitivity than this.

It appears that nobody so far has been able to measure basal level of ATP release from a single hippocampal rat slice (Wieraszko and Seyfried, 1989) or concentrations several times larger. Basal ATP release from in vitro superfused rat hypothalamic 400 μm -thick slices was measured by the luciferin-luciferase assay, but four slices were placed in one chamber and perfused continuously (Sperlagh et al., 1998). Perfusate samples were collected over a 3 min period and assayed for ATP. ATP release during resting conditions was compared with response to low and high frequency field electrical stimulation, which can be easily applied to all 4 slices. The electrical field stimulation increased the outflow of ATP more than ten-fold. That our problems were with the degree of sensitivity of the assay is demonstrated by the ouabain-evoked ATP release. The simultaneous use of six slices was necessary to detect the ATP release. One slice alone resulted in detection

problems. Unfortunately it was not feasible to arrange simultaneous injection of KCl and monitoring of the extracellular potential in four slices.

4.3 Is ATP Released During SD Wave?

The problem whether SD wave induces ATP release from nerve tissue, remained unsolved. What could be the possible mechanisms of such release?

SD is characterized by near-total depolarization of neurons and glial cells (Somjen et al., 1991). During SD neurons are unexcitable, but at the start of the depolarization and afterward bursts of impulses occur (Higachida et al., 1974; Somjen et al., 1991). This activation of neuronal activity leads to transmitter release from nerve terminals and the release of ATP which is co-stored with ACh, noradrenaline, 5-HT (Zimmermann, 1994; Vizi et al., 1997; Sperlagh et al., 1997; Sperlagh et al., 1998), or glutamate (Wieraszko et al., 1989). ATP release was usually experimentally demonstrated under more intense stimulation of nerve terminals with electrical pulses (see Introduction, 1.11). Maybe the amount of ATP released during the burst of spikes in the beginning of SD wave and afterward is not large enough to be detected, even though ATP is definitely released together with the neurotransmitters.

During SD neuronal membrane potential shifts slowly at first then becomes maximally depolarized to approximately 0 mV for 1-3 min (Somjen et al., 1991). This prolonged depolarization activates voltage-dependent Ca^{2+} channels in nerve terminals similar to the action of the depolarization caused by the action potential invading the presynaptic nerve terminal membrane. The thresholds for activation of

various calcium channels characterized at the nerve terminals vary from -40 mV to -10 mV and some of them show no voltage-dependent inactivation (Meir et al., 1999). In nerve terminals of rat hippocampal slices two types of calcium channels named N and P are described. The P type of calcium channels shows no voltage-dependent inactivation and therefore their opening allows calcium to enter the presynaptic nerve terminal during prolonged depolarization associated with SD. Upon depolarization intracellular calcium may increase substantially and gate the release of neurotransmitters (Stanley, 1997) and, therefore, the release of ATP which is co-stored with them (Zimmermann, 1997).

Extracellular amino acids were examined during SD. Concentrations of alanine, arginine, aspartate, glycine, serine, taurine and the major excitatory transmitter in the brain glutamate were increased by evoked SD (Fabricius et al., 1993). SD waves produced by 50 mM K^+ evoked a more than 3-fold increase in glutamate release (Szerb, 1991). Marked glutamate release synchronous with propagating SD waves was shown in the cerebral cortex of rats (Obrenovitch et al., 1995). The potential sources of glutamate efflux are exocytosis of neurotransmitter glutamate, the reversal of glutamate uptake and cellular swelling (Obrenovitch, 1996). All these mechanisms may contribute to glutamate release during SD.

Glutamate may be released from presynaptic vesicles by exocytosis during SD. The vesicular release of neurotransmitters is Ca^{2+} -dependent. Depolarization of neurons during SD may activate Ca^{2+} voltage-dependent channels causing Ca^{2+} influx and glutamate release by exocytosis.

In resting brain cells the levels of glutamate in the cytoplasm is around 10,000 times higher than that in the extracellular space. This gradient is maintained by glutamate carriers that present in presynaptic and glial plasma membrane. These carriers are essential for terminating the postsynaptic action of the major excitatory transmitter in the brain. The glutamate carriers are characterized by a unique coupling to Na^+ and K^+ and by a high (2-50 μM) affinity for glutamate (Kanner and Bendahan, 1982). The efficacy of glutamate transport is dependent on the Na^+/K^+ gradient across the plasma membrane. Glutamate uptake can be reversed by raising the external potassium concentration. Raising external K^+ concentration to 10 mM was sufficient to reverse glutamate uptake in glial cells isolated from the salamander retina. The glutamate uptake system in these cells has properties similar to that in mammalian glia and neurons (Statkowski et al., 1990). An outward current component produced by reversed glutamate uptake was activated by intracellular glutamate and Na^+ and increased by membrane depolarization. During SD the ion and voltage gradients favoring reversed glutamate uptake are greatly increased: (i) the extracellular potassium concentration can rise to 60-70 mM; (ii) the cells are depolarizing to 0 mV; (iii) $[\text{Na}^+]_e$ falls to 65-75 mM (see Introduction 1.2). In this situation reversed uptake will release glutamate into extracellular space contributing to the rise in extracellular glutamate concentration. The carrier could release glutamate until the extracellular glutamate concentration reaches up to 370 μM (Statkowski et al., 1990). The efflux of glutamate is of cytoplasmic origin and is Ca^{2+} -independent.

Cell swelling is a remarkable event accompanying SD wave propagation (Hansen and Zeuthen, 1981; Holthoff and Witte, 1996). It was known that swelling of primary astrocyte cultures by exposing them to hypotonic media caused release of intracellular glutamate (Kimelberg et al., 1990). The data suggested the involvement of specific transport processes rather than nonspecific opening of nonselective “holes” in the membrane. Later it has been found that the swelling-induced transport system for glutamate and other amino acids such as aspartate and taurine are related to volume-sensitive organic anion channels (VSOACs) activated by cell swelling which were found in neurons and glial cells (Pasant-Morales et al., 1994). Their experiments were designed to test the hypothesis that glutamate efflux through volume activated channels occurs during SD (Basarsky et al., 1999). SD was induced by bath application of ouabain (100 μ M) in hippocampal brain slices and was mapped by imaging intrinsic optical signals. Intrinsic optical signals provided an indirect measure of cell volume changes because cellular swelling was associated with increased light transmittance through brain slices. A significant release of glutamate during SD, even in Ca^{2+} -free solution in which conventional synaptic release is blocked, was measured. NPPB, an antagonist of VSOACs, inhibited the release of glutamate during SD. Thus, the results indicated that cellular swelling during SD causes the activation of VSOACs and the release of glutamate by permeation through these channels. VSOACs are present in the hippocampus and are likely found in both astrocytes and neurons (Kawasaki et al., 1994). Fluoroacetate, a glial metabolic poison, decreases the spontaneous efflux of glutamate during SD (Szerb, 1991) that indicate that a part of glutamate is released by glial cells. Thus,

three mechanisms may be involved in glutamate release that is observed during SD. Released glutamate, in turn, is able to activate astroglial NMDA, AMPA and kainate receptors and elicit the release of ATP from astrocytes (Queiroz et al., 1999).

There is another possible mechanism for ATP release during SD. It is known that SD wave propagation causes elevations in $[Ca^{2+}]_i$ (Hansen and Zeuthen, 1981). In the rat hippocampal slices slow $[Ca^{2+}]_i$ increase preceded a robust calcium wave that occurred concomitantly with SD wave initiated by bath application of 100 μ M ouabain (Basarsky et al., 1998). It was determined that glial cells contribute to the observed $[Ca^{2+}]_i$ dynamics by injection of the calcium indicator calcium orange into astrocytes. Calcium waves were observed associated with SD confirming that part of $[Ca^{2+}]_i$ increase was of astrocytic origin. As discussed in Introduction 1.10 there were experiments that established that medium collected from astrocyte cultures during (but not before) calcium wave stimulation contained ATP (Guthrie et al., 1999). The release of ATP by astrocytes during a calcium wave did not depend on the type of stimulation used in experiments to evoke calcium waves. Electrical and mechanical stimulation produced the same effect. The stimulated cells expressing the calcium wave released ATP into the medium which evoked calcium response in adjacent astrocytes that in turn released ATP which stimulated calcium wave in their neighbors. Therefore it is possible that calcium waves that occur during SD cause the release of ATP from astrocytes.

It is not unreasonable to propose that final concentration of ATP in extracellular space after all these events during SD wave propagation is elevated

high enough to activate microglial cells but was not sufficient for detection in our experiments.

5. CONCLUSIONS

The following conclusions can be made:

1. During ouabain-evoked SD waves ATP is released. However due to the possibility that application of ouabain by itself may cause the release of ATP, rather than SD, this finding alone is not sufficient to conclude that SD waves cause the release of ATP.
2. During SD wave elicited by K^+ injection and propagating across a single hippocampal slice we were not able to detect ATP release because the sensitivity of luciferin-luciferase system was not sufficient to measure the basal ATP efflux and its changes.
3. Manipulations involving inhibition of ATP degradation, improvement of the experimental chamber, and concentration of the effluent did not improve the sensitivity of the assay.
4. Our results, however suggest that 2/3 of any amount of ATP released by cells in the brain slices are degraded by ecto-enzymes.

6. REFERENCES

- Abraham E. H., Prat A. G., Gerweek L., Seneveratne T., Arceci R. J., Kramer R., Guidotti G., and H. F. Cantiello. The multidrug resistance (mdr 1) gene product functions as an ATP channel. *Proc. Natl. Acad. Sci. USA.* 90: 312-316, 1993.
- Aitken P. G., Jing I., Young J., and G. G. Somjen. Ion channel involvement in hypoxia-induced spreading depression in hippocampal slices. *Brain Res.* 541: 7-11, 1991.
- Altman J. Microglia emerge from the fog. *TINS.* 17(2): 47 – 49, 1994.
- Astrup J., Symon L., and B. K. Siesjo. Thresholds in cerebral ischemia: the ischemic penumbra. *Stroke.* 12: 723 – 725, 1981.
- Astrup J., Symon L., and N. M. Branston. Cortical evoked potential and extracellular K^+ and H^+ at critical levels of brain ischemia. *Stroke.* 8: 51 – 57, 1977.
- Banati R. B., Gehrmann J., Schubert P., and B. W. Kreutzberg. Cytotoxicity of microglia. *Glia.* 7: 111 – 118, 1993.
- Basarski T. A., Feighan D., and B. A. MacVicar. Glutamate release through volume-activated channels during spreading depression. *J. Neurosci* 19(15): 6439 – 45, 1999.
- Basarski T. A., Steven N. D., Andrew R. D., and B. A. MacVicar. Imaging spreading depression and associated intracellular calcium waves in brain slices. *J. Neurosci.* 18: 7189-7199, 1998.
- Berridge M. J. Capacitative calcium entry. *Biochem. J.* 312: 1 – 12, 1995.
- Bures J., Buresova O., and J. Krivanek. The mechanism and application of Leao's spreading depression of electroencephalographic activity. Academic. New York. 1974.
- Burnstock G., Campbell G., Satchell D. and A. Smythe. Evidence that adenosine triphosphate or a related nucleotide is the transmitter substance released by non-adrenergic inhibitory nerves in the gut. *Br. J. Pharmac.* 40: 668-688, 1970.
- Busa W. B., and R Nuccitelli. Metabolic regulation via intracellular pH. *Am. J. Physiol.* 246: R409 – R438, 1984.

- Busija D. W., and W. Meng. Retention of cerebrovascular dilation after cortical spreading depression in anesthetized rabbits. *Stroke*. 24(II): 1740 – 4, 1993.
- Caciagli F., Ciccarelli R., Di Iorio P., Ballerini P., and L. Tacconelli. Cultures of glial cells release purines under field electrical stimulation: the possible ionic mechanisms. *Pharmacol. Res. Commun.*, 20: 935-47, 1988.
- Chen Q., Chopp M., Bodzin G., and H. Chen. Temperature modulation of cerebral depolarization during focal cerebral ischemia in rats. *J. Cereb. Blood Flow Metab.* 13: 389 – 394, 1993.
- Chesler W., and R. P. Kraig. Intracellular pH transients of mammalian astrocytes. *J. Neurosci.* 9(6): 2011-2019, 1989.
- Collins F., Schmidt M. F., Guthrie P. B., and S. B. Kater. Sustained increase in intracellular calcium promotes neuronal survival. *J. Neurosci.* 11: 2582 – 2587, 1991.
- Collo G., Neidhart S., Kawashima E., Kosco-Vilbois M., North R. A., and G. Buell. Tissue distribution of the P2X₇ receptor. *Neuropharmacology*. 36(9): 1277 – 1283, 1997.
- Colonna D. M., Meng M. W., Deal D., and D. W. Busija. Nitric oxide promotes arteriolar dilation during cortical spreading depression in rabbits. *Stroke*. 25: 2463-2470, 1994.
- Colonna D. M., Meng W., Deal D., and D. W. Busija. Calcitonin gene-related peptide promotes cerebrovascular dilation during cortical spreading depression in rabbits. *Am. J. Physiol.* 266 (Heart Circ Physiol. 35): H1095-H1102, 1994.
- Csiba L., Paschen W., and G. Mies. Regional changes in tissue pH and glucose content during cortical spreading depression in rat brain. *Brain Res.* 336: 167 – 170, 1985.
- Dani J. W., Chernjavsky A., and S. J. Smith. Neuronal activity triggers calcium waves in hippocampal astrocyte networks. *Neuron*. 8: 429-440, 1992.
- Denburg J. L. and W. D. McElroy. Anion inhibition of firefly luciferase. *Arch. Biochem. Biophys.* 141: 668-675, 1970.
- Dietrich W. D., Feng Z.-C., Leistra H., Watson B. D., and M. Rosenthal. Photothrombotic infarction triggers multiple episodes of cortical spreading depression in distant brain regions. *J. Cereb. Blood Flow Metab.* 14:20-28, 1994.

- Dunwiddie T., Diao L., and W. R. Proctor. Adenin nucleotides undergo rapid, quantitative conversion to adenosine in the extracellular space in rat hippocampus. *J. Neurosci.* 17(20): 7673-7682, 1997.
- Edwards F. A. and A. J. Gibb. ATP-a fast neurotransmitter. *FEBS.* 325: 86-89, 1993.
- Fabricsius M., Jensen L. H., and M. Lauritzen. Microdialysis of interstitial amino acids during spreading depression and anoxic depolarization in rat neocortex. *Brain Res.* 612: 61 – 69, 1993.
- Ferrari D., Villaba M., Chiozzi P., Falzoni S., Ricciardi-Castagnoli P., and F. D. Virgilio. Mouse microglial cells express a plasma membrane pore gated by extracellular ATP. *J. Immunol.* 156: 1531 – 1539, 1996.
- Gehrmann J., Mies G., Bonnekoh P., Banati R., Iljima T., and G. W. Kreutzberg. Microglial reaction in the rat cerebral cortex induced by cortical spreading depression. *Brain Pathol.* 3: 11 – 17, 1993.
- Gehrmann J., Banati R. B., Wiessner C., Hossmann K. A., and Kreutzberg G. W. Reactive microglia in cerebral ischemia: an early mediator of tissue damage? *Neuropathol Appl Neurobiol.* 21: 277 – 289, 1995.
- Ghosh A. and M. E. Greenberg. Calcium signaling in neurons: molecular mechanisms and cellular consequences. *Science.* 268: 239 – 247, 1995.
- Gilles R., Pequeux A., Saive J. J., Spronck A. C., and G. Thome-Lentz. Effect of various ions on ATP determinations using the “luciferine-luciferase” system. *Arch. Int. Physiol. Biochem.* 84(4): 807-817, 1976.
- Gjedde A., Hansen A. J., and B. Quistorff. Blood-brain glucose transfer in spreading depression. *J. Neurochem.* 37(4): 807 – 812, 1981.
- Goodsby P. J., Kaube J. H., and K. L. Hoskin. Nitric oxide synthesis couples cerebral blood flow and metabolism. *Brain Res.* 595: 167-170, 1992.
- Gualt L. M., Lin C. W., LaManna J. C., and W. D. Lust. Changes in energy metabolites, cGMP and intracellular pH during cortical spreading depression. *Brain Res.* 641: 176 – 180, 1994.
- Guthrie P. B., Knappenberger J., Segal M., Bennett M. V. L., Charles A. C., and S. B. Kater. ATP released from astrocytes mediates glial calcium waves. *J. Neurosci.* 19: 520-528, 1999.
- Haas S., Brockhaus J., Verckhratsky A., and H. Kettenmann. ATP-induced membrane currents in amoeboid microglia acutely isolated from mouse brain slices. *Neurosci.* 75(1): 257 – 261, 1996.

- Haas S., Brockhaus J., Verkhatsky A., and H. Kettenmann. ATP-induced membrane currents in amoeboid microglia acutely isolated from mouse brain slices. *Neurosci.* 75(1): 257 – 261, 1996.
- Hagland M. M. and P.A. Schwartzkroin. Role of Na-K pump potassium regulation and IPSPs in seizures and spreading depression in immature rabbit hippocampal slices. *J. Neurophysiol.* 63: 225 – 239, 1990.
- Hakim A. M. Ischemic penumbra. The therapeutic window. *Neurology.* 51 (Suppl 3): S44 – S46, 1998.
- Hakim A. M. The cerebral ischemic penumbra. *Can. J. Neurol. Sci.* 14: 557 – 559, 1987.
- Hansen A. J. and C. E. Olsen. Brain extracellular space during spreading depression and ischemia. *Acta Physiol. Scand.* 108: 355-365, 1980.
- Hansen A.J., and T. Zeuthen. Extracellular ion concentration during spreading depression and ischemia in the rat brain cortex. *Acta Physiol. Scand.* 113: 437-445, 1981.
- Hansen A. J., Quistorf B., and A. Gjedde. Relationship between local changes in cortical blood flow and extracellular K^+ during spreading depression. *Acta. Physiol. Scand.* 109: 1-6, 1980.
- Herriras O. and G. G. Somjen. Analysis of potential shifts associated with recurrent spreading depression and prolonged unstable spreading depression induced by microdialysis of elevated K^+ in hippocampus of anesthetized rats. *Brain Res.* 610: 283-294, 1993.
- Higashida H., Mitarai G. and S. Watanabe. A computational study of membrane potential changes in neurons and neuroglial cells during spreading depression in the rabbit. *Brain Res.* 65: 411-425, 1974.
- Holthoff K. and O. W. Witte. Intrinsic optical signals in rat neocortical slices measured with near-infrared dark-field microscopy reveal changes in extracellular space. *J. Neurosci.* 16(8): 2740-9, 1996.
- Hossmann K-A. Viability thresholds and the penumbra of focal ischemia. *Ann. Neurol.* 36: 557 – 565, 1994.
- Inoue K., Koizumi S., and K. Nakazawa. Glutamate-evoked release of adenosine-5'-triphosphate causing an increase in intracellular calcium in hippocampal neurons. *NeuroReport.* 6: 437-40, 1995.

- Inoue K., Nakajima K., Morimoto T., Kikuchi Y., Koizumi S., Illes P., and S. Kohsaka. ATP stimulates Ca^{2+} -dependent plasminogen release from cultured microglia. *Br. J. Pharmacol.* 123: 1304 – 1310, 1998.
- Jabs R., Bekar L. K., and W. Walz. Reactive astrogliosis in the injured and postischemic brain. From: *Cerebral Ischemia: Molecular and Cellular Pathophysiology*. Edited by: W. Walz. Humana Press Inc., Totowa, N. J. p. p. 233 – 249, 1999.
- Jing J., Aitken P. G., and G. Somjen. Role of calcium channels in spreading depression in rat hippocampal slices. *Brain Res.* 604: 251-259, 1993.
- Kanner B. I. and A. Bendahan. Binding order of substrates to the sodium and potassium ion coupled L-glutamic acid transporter from rat brain. *Biochem.* 21: 6327-6330, 1982.
- Kawasaki M., Uchida S., Monkawa T., Miyawaki A., Mikoshiba K., Marumo F. and S. Sasaki. Cloning and expression of a protein kinase C-regulated chloride channel abundantly expressed in rat brain neuronal cells. *Neuron.* 12: 597-604, 1994.
- Kimelberg H. K., Goderie S. K., Higman S., Pang S., and R. A. Waniewski. Swelling-induced release of glutamate, aspartate, and taurine from astrocyte cultures. *J. Neurosci.* 10(5): 1583 – 1591, 1990.
- Kobayashi S., Harris V. A., and F. A. Welsh. Spreading depression induces tolerance of cortical neurons to ischemia in rat brain. *J. Cereb. Blood Flow Metab.* 15: 721 – 727, 1995.
- Kraig R. P., and C. Nicholson. Extracellular ionic variations during spreading depression. *Neuroscience.* 3: 1045 – 1059, 1978.
- Kraig R. P., Dong L., Thisted R., and C. B. Jaeger. Spreading depression increases immunohistochemical staining of glial fibrillary acidic protein. *J. Neurosci.* 11: 2187 – 2198, 1991.
- LaManna J. C., and M. Rosenthal. Effect of ouabain and phenobarbital on oxidative metabolic activity associated with spreading cortical depression in cats. *Brain Res.* 88: 145 – 149, 1975.
- Langosch J. M., Gebicker-Harter P. J., Norenberg W. and P. Illes. Characterization and transduction mechanisms of purinoreceptors in activated rat microglia. *Br. J. Pharmacol.* 113: 29 – 34, 1994.

- Largo C., Ibarz J. M., and O.Herrars. Effects of the gliotoxin fluorocitrate on spreading depression and glial membrane potential in rat brain in situ. *J. Neurophysiol.* 78:295-307, 1997.
- Largo C., Tombaugh G. C., Aitken P. A., Herreras O., and G. G. Somjen. Heptanol but not fluoroacetate prevents the propagation of spreading depression in rat hippocampal slices. *J. Neurophysiol.* 77: 9-16, 1997.
- Leao A. Spreading depression of activity in the cerebral cortex. *J. Neurophysiol.* 7: 359-390, 1944.
- Lees G. J. and Leong W. Brain lesions induced by specific and non-specific inhibitors of sodium-potassium ATPase. *Brain Res.* 649: 225 – 233, 1994.
- Lees G. J. Inhibition of sodium-potassium-ATPase: a potentially ubiquitous mechanism contributing to central nervous system neuropathology. *Brain Res. Rev.* 16: 283 – 300, 1991.
- Lees G. J., Lehmann A., Sanberg M., and Hamberger A. The neurotoxicity of ouabain, a sodium-potassium ATPase inhibitor, in the rat hippocampus. *Neurosci. Lett.* 120: 159 – 162, 1990.
- Lehrmann E., Christensen T., Zimmer J., Diemer N. H., and B. Finsen. Microglial and macrophage reactions mark progressive changes and define the penumbra in the rat neocortex and striatum after transient middle cerebral artery occlusion. *J. Comp. Neurol.* 386: 461 – 467, 1997.
- Lothman E., LaManna J., Cordingley G., Rosenthal M., and G. Somjen. Responses of electrical potential, potassium levels, and oxidative metabolic activity of the cerebral neocortex of cats. *Brain Res.* 88: 15-36, 1975.
- Mark R. J., Hensley K., Butterfield D. A., and M. P. Mattson. Amyloid β -peptide impairs ion-motive ATPase activities: evidence for a role in loss of neuronal Ca^{2+} homeostasis and cell death. *J. Neurosci.* 15(9): 6239 – 49, 1995.
- Marrannes R., Willems R., De Prins E. and Wauquier A. Evidence for a role of the N-methyl-D-aspartate (NMDA) receptor in cortical spreading depression in the rat. *Brain Res.* 457: 226-240, 1998.
- Matsushima K., Hogan M. J., and A. M. Hakim. Cortical spreading depression protects against subsequent focal cerebral ischemia in rats. *J. Cereb. Blood Flow Metab.* 16: 221 – 226, 1996.
- McLarnon J. G., Zhang L., Goghari V., Lee Y. B., Walz W., Krieger C., and S. U. Kim. Effects of ATP and elevated K^+ on K^+ currents and intracellular Ca^{2+} in human microglia. *Neurosci.* 91(1): 343 – 352, 1999.

- Meir A., Ginsburg S., Butkevich A., Kachaksky S. G., Kaiserman I., Ahdut R., Demirgoren S., and R. Rahamimoff. Ion channels in presynaptic nerve terminals and control of transmitter release. *Physiol. Rev.* 79(3): 1019-88, 1999.
- Memezawa H., Smith M. L., and B. K. Siesjo. Penumbra tissues salvaged by reperfusion following middle cerebral artery occlusion in rats. *Stroke.* 23: 552 – 559, 1992.
- Mies G., and W. Paschen. Regional changes in blood flow, glucose, and ATP content determined on brain sections during a single passage of spreading depression in rat brain cortex. *Exp Neurol.* 84: 249 – 258, 1984.
- Mies G., Iljima T., and K. A. Hossmann. Correlation between peri-infarct DC shifts and ischemic neuronal damage in rats. *Neuroreport* 4: 709 – 711, 1993.
- Monoteith G. R. and M. P. Blaustein. Different effects of low and high dose cardiotonic steroids on cytosolic calcium in spontaneously active hippocampal neurons and in co-cultured glia. *Brain Res.* 795: 325 – 40, 1998.
- Nedergaard M. Spreading depression as a contributor to ischemic brain damage. *Adv. Neurol.* 71: 75 – 84, 1996.
- Nedergaard M. and J. Astrup. Infarct rim: effect of hyperglycemia on direct current potential and (14C)-deoxyglucose phosphorylation. *J. Cereb. Blood Flow Metab.* 6: 607 – 615, 1986.
- Nedergaard M., Cooper A. J. L., and S. A. Goldman. Gap junctions are required for the propagation of spreading depression. *J. Neurobiol.* 28: 433-444, 1995.
- Nedergaard M. and N. H. Diemer. Focal ischemia of the rat brain with special reference to the influence of plasma glucose concentration. *Acta. Neuropathol.* 73: 131 – 137, 1987.
- Nedergaard M. and A. J. Hansen. Spreading depression is not associated with neuronal injury in the normal brain. *Brain Res.* 449: 395 – 398, 1988.
- Nedergaard M. and A. J. Hansen. Characterization of cortical depolarization evoked in focal cerebral ischemia. *J. Cereb. Blood Flow Metab.* 13: 568 – 574, 1993.
- Norenberg W., Langosch J. M., Gebicke-Haerter P. J., and P. Illes. Characterization and possible function of adenosine 5'-triphosphate receptors in activated rat microglia. *Br. J. Pharmacol.* 111: 942 – 950, 1994.

- Obrenovitch T. P. Origins of glutamate release in ischemia. *Acta Neurochir.* [Suppl]. 66: 50 – 55, 1996.
- Obrenovitch T. P., Zilkha E., and J. Urenjak. Evidence against high extracellular glutamate promoting the elicitation of spreading depression by potassium. *J. Cereb. Blood Flow Metab.* 160: 923-931, 1996.
- Obrenovitch T. P., Zilkha E., and J. Uzenjak. Intracerebral microdialysis: electrophysiological evidence of a critical pitfall. *J. Neurochem.* 64: 1884 – 1887, 1995.
- Obrenovitch T.P. and E. Zilcha. High extracellular potassium, and not extracellular glutamate is required for the propagation of spreading depression. *J. Neurophysiol.* 73: 2107-2114, 1995.
- Philips J. W., Walter G. A., O'Regan M. H., and R. E. Stair. Increases in cerebral cortical perfusate adenosine and inosine concentrations during hypoxia and ischemia. *J. Cereb. Blood Flow Metab.* 7: 679 – 686, 1987.
- Phillips J. M., and C. Nicholson. Anion diffusion in spreading depression investigated with ion-sensitive microelectrodes. *Brain Res.* 173: 567- 571, 1979.
- Phillips J. W., O'Regan M.H., and L.M. Perkins. Adenosine 5'-triphosphate release from the normoxic and hypoxic in vivo rat cerebral cortex. *Neurosci.Lett.* 151: 94-96, 1993.
- Queiroz G., Meyer D.K., Meyer A., Starke K., and I. Von Kugelgen. A study of the mechanism of the release of ATP from rat cortical astroglial cells evoked by activation of glutamate receptors. *Neurosci.* 91(3): 1171 – 81, 1999.
- Queiroz G., Gebiske-Haerter P. J., Schobert A., Starke K., and I. V. Kugelgen. Release of ATP from cultured rat astrocytes elicited by glutamate receptor activation. *Neurosci.* 78(4): 1203-1208, 1997.
- Rawanduzy A., Hansen A., Hansen T. W., and M. Nedergaard. Effective reduction of infarct volume by gap junction blockade in a rodent model of stroke. *J. Neurosurg.* 87(6): 916 – 20, 1997.
- Richerson, G. B. and C. Messer. Effect of composition of experimental solutions on neuronal survival during rat brain slicing. *Exp. Neurol.* 1331: 133 – 143, 1995.
- Ruppin E., Ofer E., Reggia Y. A, Revett K., and S. Goodall. Pathogenic mechanisms in ischemic damage: a computational study. *Comput. Biol. Med.* 29: 39 – 59, 1999.

- Schoeter M., Schiene K., Kraemer M., Haggemann G., Weigel H., Eysel U. T., Witte O. W., and G. Stoll. Astroglial responses in photochemically induced focal ischemia of the rat cortex. *Expl. Brain Res.* 106: 1 – 6, 1995.
- Schroeter M., Jander S., Witte O. W., and G. Stoll. Heterogeneity of the microglial response in photochemically induced focal ischemia of the rat cerebral cortex. *Neuroscience.* 89(4): 1367 – 1377, 1999.
- Seardown M. J. The triggering of spreading depression in the chicken retina: a pharmacological study. *Brain Res.* 607: 189-194, 1993
- Shibata M., Leffer C. W., and D. W. Busija. Pial arteriolar constriction following cortical spreading depression is mediated by prostanoids. *Brain Res.* 572: 190 –197, 1992.
- Shibata M., Leffler C. W., and D.W. Busija. Cerebral hemodynamics during cortical spreading depression in rabbits. *Braing Res.* 530: 267-274, 1990.
- Shinohara M., Dollinger B., and G. Brown. Cerebral Glucose utilization: local changes during and after recovery from spreading cortical depression. *Science.* 23: 188-190, 1979.
- Snow R. W., Taylor C. P., and F. E. Dudek. Electrophysiological and optical changes in slices of rat hippocampus during spreading depression. *J. Neurophysiol.* 50: 561-572, 1983.
- Somjen G. G., Aitken P. G., Czeh C. L., Herreras O., Jing J., and J.N. Young. Mechanisms of spreading depression: a review of recent findings and a hypothesis. *Can. J. Physiol. Pharmacol.* 70: S248-S254, 1992.
- Sperlgh B., Andras I., and E. S. Vizi. Effect of subtype-specific Ca^{2+} -antagonists and Ca^{2+} -free media on the field stimulation-evoked release of ATP and [^3H]acetylcholin from rat habenula slices. *Neurochemical Res.* 22(8): 967-975, 1997.
- Sperlgh B., Sershen H., Lajtha A. and E. S. Vizi. Co-release of endogenous ATP and [^3H]noradrenaline from rat hypothalamic slices: origin and modulation by α_2 -adrenoceptors. *Neurosci.* 82(2): 511-520, 1998.
- Stahl W. L. ($\text{Na}^+ + \text{K}^+$)-ATPase: function, structure and conformations. *Annu. Neurol.* 16: S121 – S127, 1984.
- Stanley E. F. The calcium channel and the organization of the presynaptic transmitter release face. *Trends Neurosci.* 20: 404 – 409, 1997.

- Steinberg T. H., Newman A. S., Swanson J. A., and S. C. Silverstein. ATP⁴⁻ permeabilizes the plasma membrane of mouse macrophages to fluorescent dyes. *J. Biol. Chem.* 262: 8884 – 8888, 1987.
- Surprenant A., Rassendren F., Kawashima E., North R. A., and G. Buell. The cytolytic P2Z receptor for extracellular ATP identified as a P2X receptor (P2X₇). *Science*. 272: 735 – 738, 1996.
- Sweadner K. J. Isozymes of the Na⁺/K⁺-ATPase. *Biochem. Biophys. Acta*. 988: 185 – 220, 1989.
- Sweeney M., Yager J. Y., Walz W., and B.H.J. Juurlink. Cellular mechanisms involved in brain ischemia. *Can. J. Physiol. Pharmac.* 73: 1525 – 1535, 1995.
- Szatkowski M., Barbour B., and D. Attwell. Non-vesicular release of glutamate from glial cells by reversed electrogenic glutamate uptake. *Nature*. 348:443-446, 1990.
- Szerb J. C. Glutamate release and spreading depression in the fascia dentata in response to microdialysis with high K⁺: role of glia. *Brain Res.* 542(2): 259 – 65, 1991.
- Takano K., Latour L. L., Formato J. E., Carano R. A. D., Helmer K. G., Hasegawa Y., Sotak C. H., and M. Fisher. The role of spreading depression in focal ischemia evaluated by diffusion mapping. *Ann. Neurol.* 39(3): 308 – 18, 1996.
- Tobiasz C., and C. Nicholson. Tetrodotoxin-resistant propagation and extracellular sodium changes during spreading depression in rat cerebellum. *Brain Res.* 241: 329-33, 1982.
- Toescu E. C., Moller T., Kettenmann H. and A. Verkhratsky. Long-term activation of capacitative Ca²⁺ entry in mouse microglial cells. *Neurosci.* 86(3): 925 – 935, 1998.
- Vizi E. S., Liang S. D., Sperlagh B., Kittel A. and Z. Juranyi. Studies on the release and extracellular metabolism of endogenous ATP in rat superior cervical ganglion: support for neurotransmitter role of ATP. *Neurosci.* 79(3): 893-903, 1997.
- Walz W. and E. Hinks. Carrier-mediated KCl accumulation accompanied by water movements is involved in the control of physiological K⁺ levels by astrocytes. *Brain Res.* 343: 44-51, 1985.
- Walz W. Induction of reactive gliosis by purinoceptor activation: a critical appraisal. *Kaohsiung J. Med. Sci.* 13: 30 – 35, 1997.

- Walz W., Ilshner S., Ohlemeyer C., Banati R., and H. Kettenmann. Extracellular ATP activates a cation conductance and a K⁺ conductance in cultured microglial cells from mouse brain. *J. Neurosci.* 13(10): 4403 – 4411, 1993.
- Wet J. R., Wood K. V., Deluca M., Helinski D. R., and S. Subramani. Firefly luciferase gene: structure and expression in mammalian cells. *Mol. Cell. Biol.* 7: 725-737, 1987.
- White T. D. and W. F. MacDonald. Neural release of ATP and adenosine. *Ann. N.Y. Acad. Sci.* 603: 287-98, 1990.
- White T. D. Direct detection of depolarization-induced release of ATP from a synaptosomal preparation. *Nature.* 267: 67-68, 1977.
- White T. D. Release of ATP from a synaptosomal preparation by elevated extracellular K⁺ and by veratridine. *J. Neurochem.* 30: 329-336, 1978.
- Wieraszko A. and T. N. Seyfried. Increased amount of extracellular ATP in stimulated hippocampal slices of seizure prone mice. *Neurosci. Lett.* 106: 287 – 293, 1989.
- Wieraszko A., Goldsmith G. and T. N. Seyfried. Stimulation-dependent release of adenosine triphosphate from hippocampal slices. *Brain Res.* 485: 244-250, 1989.
- Wood P. L. Microglia as a unique cellular target in the treatment of stroke: potential neurotoxic mediators produced by activated microglia. *Neurol. Res.* 17: 242 – 248, 1995.
- Zimmermann H. Signaling via ATP in the nervous system. *TINS.* 17(10): 420-426, 1994.